"FEDERICO II"
UNIVERSITY OF NAPLES

SCHOOL OF MEDICINE

PhD PROGRAM IN NEUROSCIENCE

XXVI CYCLE

Preclinical studies exploring the therapeutic potential of K_v7 potassium channels in CNS diseases

Coordinator:
PROF. LUCIO ANNUNZIATO

Tutor:
PROF. MAURIZIO TAGLIALATELA

PhD Student:
VINCENZO BARRESE

Academic Year 2013-2014

INDEX

INTRODUCTION

Ionic homeostasis is a pivotal process in the regulation of cell metabolism, in particular for excitable cells such as neurons. Alterations of ionic balance are common in different pathologic conditions, such as brain ischemia or epilepsy. For instance, modifications in cytosolic and subcellular calcium ions (Ca^{2+}) dynamics have been indicated as main pathways underlying ischemic neuronal death; moreover, Na^+, K^+ and Cl^- imbalances seem to play an important role in regulating cell survival. Indeed, ion channels - apart from their well-known role in determining neuronal firing- can regulate different cellular proteins and processes, such as kinases, transcription factors, mitochondrial function and free radical formation (Arumugan et al., 2009). Among the different ion species, potassium (K^+) seems to play a primary role in the regulation of neuronal cell death/survival. Indeed, growing evidence demonstrate that low intracellular K^+ concentrations ($[K^+]_i$) lead to apoptosis in neurons, either with an indirect- (Cl^- and water outflow, cell shrinkage, mitochondrial swelling and subsequent induction of pro-apoptotic signals) or with a direct- mechanism (activation of nucleases and caspases, normally inhibited by high $[K^+]_i$ levels) (Leung, 2010).

$[K^+]_i$ are strictly regulated by different classes of both voltage-dependent and -independent K^+ channels; therefore, modulation of the activity of such relevant class of membrane proteins can affect cell fate. Indeed, pharmacological blockade of K^+ channels (induced by exposure to drugs such as tetraethylammonium, TEA), or reduction of the driving force for K^+ (obtained by an increase of $[K^+]_e$) lead to a decrease in $[K^+]_i$ outflow from the cell and to a reduction of neuronal death in different in vitro models of neuronal damage, such as serum deprivation (Yu et al., 1997) or toxic β-amyloid fragments exposure (Colom et al., 1998). An increased expression or activity of different classes of K^+ channels seems to be an early event in several in vitro models of neurotoxicity (Pannaccione et al., 2005 and 2007). On the other hand, it should be mentioned that a decreased expression/function of some subclasses of K^+ channels causes neuronal hyper-excitability, thus promoting apoptotic neuronal death (Henshall and Simon, 2005). In this view, K^+ channels-activating drugs, by

reducing neuronal excitability and subsequent energy loss, might represent a useful tool to prevent neuronal cell death.

This dual role exerted by K^+ in neuronal survival might depend on the differential function of distinct classes of voltage-dependent K^+ channels, each showing peculiar subcellular location, biophysical properties, modulation by second messengers, and pharmacological profile (Leung et al., 2010).

Potassium channels classification

Potassium channels are a heterogeneous and ubiquitous family of proteins, encoded by more than 78 genes in human (Wulff et al., 2009). They are transmembrane proteins able to selectively conduct K^+ ions across the phospholipidic bilayer with a very high flow rate (10^6-10^8/ions/s), in a direction determined by the electrochemical gradient (driving force). Such specific and fast process is made possible by particular features of these proteins, namely: 1) a pore with a selectivity filter, that allow only K^+ ions to flow across the cell membrane; 2) a gating mechanism, allowing the channel to open or close; the stimulus determining the gating can be various (ligand-binding, changes in membrane potential, variations in intracellular Ca^{2+} concentrations) but usually specific for each channel.

Since the reversal potential for K^+ is more negative than cell membrane resting potential, K^+ ions flow is commonly outward; thus, K^+ channels cause a re- or a hyper-polarization of the cell, thus stabilizing membrane potential and reducing cell excitability.

The first gene encoding for a K^+ channel was cloned in 1987 from a Drosophila mutant called Shaker, because of the fruit fly characteristic behavior under ether anesthesia (Papazian et al., 1987). Other three members of K^+ channel family (called Shab, Shaw and Shal) were cloned from the same genome, opening the door to the subsequent cloning of more than 200 genes in different species encoding for K^+ channels. Based on the aminoacidic sequence and on gating properties, K^+ channels are usually classified in three subfamily:

- *Inward rectifier K^+ channels with one pore and two transmembrane domains (K_{ir})*: these channels are formed by two transmembrane domains and a pore loop between, that usually assemble in tetramers, although more complex arrangements have been described (Shieh et al., 2000). Members of this family are called inward rectifier because of their ability to conduct current mainly in the inward direction, thus contributing in setting membrane resting potential. This property is attributed to gating mechanisms in which internal Mg^{2+} and polyamines occlude access of K^+ ions to the inner part of the pore (Matsuda, 1991; Ficker et al., 1994). The pathophysiological relevance of these channels is underlined by diseases caused by mutations in the genes encoding for members of K_{ir} family. For instance, mutations in $K_{ir}1.1$ (KCNJ1 o ROMK) are responsible for Bartter Syndrome (Simon et al., 1996), characterized by salt wasting from the renal tubules, mainly the thick ascending loop of Henle. Moreover, alteration in kcnj2 are linked in 60% of cases to Andersen-Tawil Syndrome, a disorder that causes periodic paralysis, arrhythmia and developmental abnormalities (Bendahhou et al, 2005), while kcnj11 gene defects are associated to congenital hyperinsulinism and permanent neonatal diabetes mellitus (Bennett et al., 2010).
- *K^+ channels containing four transmembranes with two pore regions (K_{2P}).* The first member of this family to be identified in mammals was called TWIK1 (Tandem of P-domains in a Weak Inward Rectifying K channel); as other channels of this family, K_{2P} do assemble in dimers and are commonly regulated by various stimuli, such as mechanical stress and arachidonic acid KCNK2, KCNK4 and KCNK10), protein kinase C and low pH (KCNK1 and KCNK6) or hypoxia (KCNK3 and KCNK9). Moreover, K_{2P} channels in central nervous system are activated by volatile anesthetics like halothane, thus contributing to neurons "silencing" (Gruss et al, 2004). Although no disease-causing mutation has been found in genes encoding for these channels, it has been suggested that members belonging to K_{2P} group participate in the regulation of different pathophysiologic processes such as electrolytes transport in the kidney,

general anesthesia, pain, main depression and neuroprotection (Heitzmann e Warth, 2008).

- *Voltage-gated K^+ channels containing six (Shaker-like, K_v) or seven (Slo-like, K_{Ca}) transmembrane domains with one pore.* This group comprises K^+ channels activated by membrane depolarization, divided in 12 sub-families by sequence homology criteria and named K_v1- K_v12 (Gutman et al., 2005). They are formed by six transmembrane domains (called S1-S6), with segment S1-S4 forming the voltage-sensing domain (VSD) and the S5-S6 region making up the pore. Among them, K_v1- K_v4 are the typical voltage-gated K^+ channel, showing high similarity to their orthologous in Drosophila (Shaker, Shab, Shaw, Shal, respectively); subsequent genomic studies led to the cloning of the other eight subfamily, some of them strictly related to their own orthologous channel in Drosophila, such as K_v7 (KCNQ), K_v10 (Eag) K_v11 (Erg), K_v12 (Elk). K_v5, K_v6, K_v8 e K_v9 families do not underlie any K^+ conductance, but they do regulate the expression and the biophysical properties of other subunits they are assembled with. K_{Ca} channels are slightly different from the other members of this group, since they have an additional transmembrane segment (called S0) and channel gating regulated also by intracellular calcium levels; this ability is due to a C-terminal cytoplasmic domain able to sense calcium levels (named calcium bowl) in high conductance channels (BK), or to the strict interaction with calmodulin (intermediate or small conductance channels, IK/SK; Fanger et al, 1999).

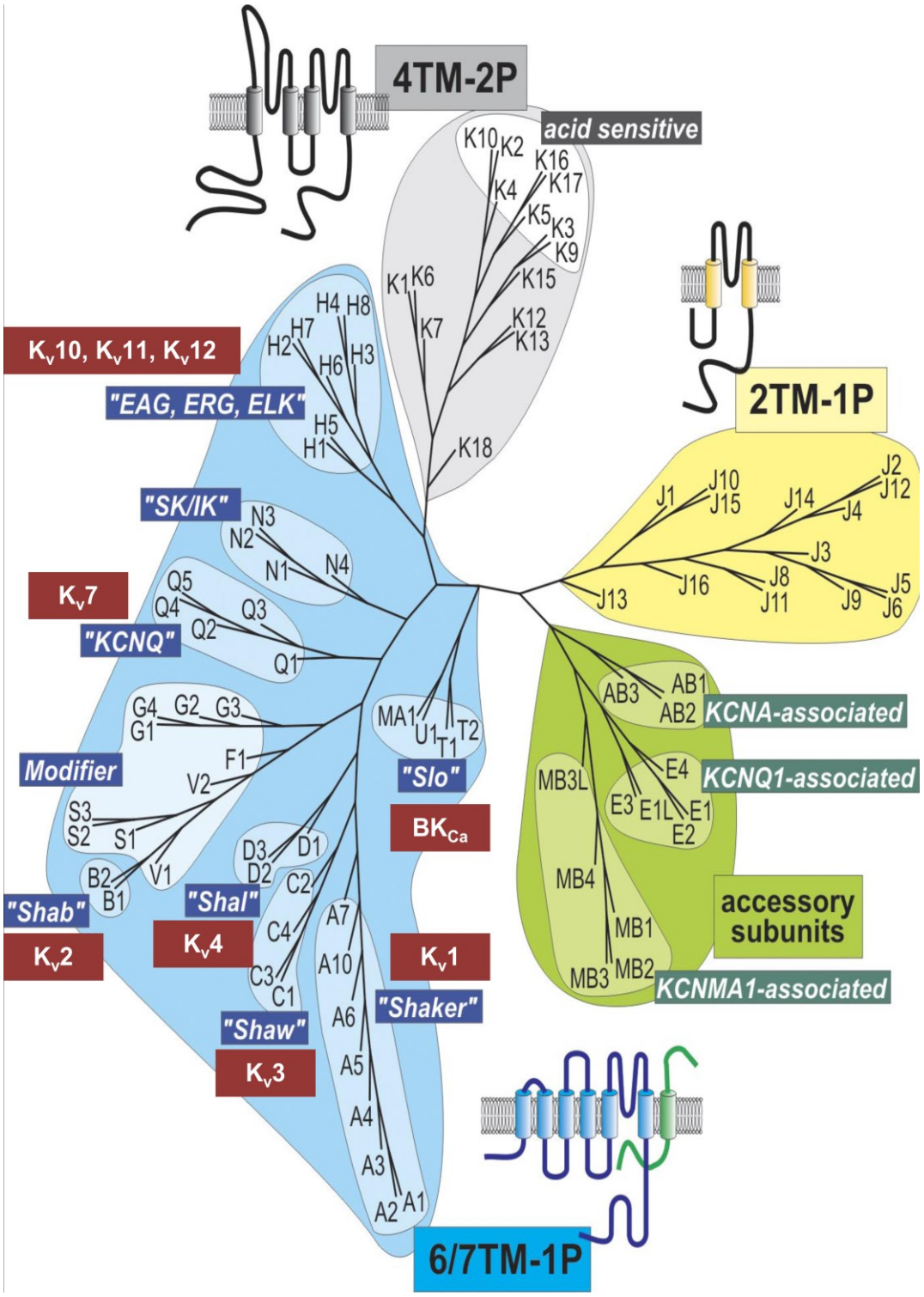

Figure 1. Potassium channels classification.

As for other ion channels, main pore-forming K^+ channels subunits (called α subunit) can be assembled to accessory subunits which can regulate their activity, subcellular localization and interaction with other proteins and cellular

structure, such as cytoskeleton or extracellular matrix (Isom et al., 1994). For instance, KchAP regulates the expression and function of $K_v2.1$, $K_v1.3$ and $K_v4.3$ (Kuryshev et al, 2000), while different β subunits can modulate the activity and toxin-sensitivity of BK_{Ca} channels (Brenner et al., 2000); moreover, sulfonylurea receptor (SUR) confers nucleotide sensitivity to inward rectifier $K_{ir}6.1$ e $K_{ir}6.2$ (Aguilar-Bryan et al, 1995), whereas minK subunit modifies biophysical properties of $K_v7.1$ (Sanguinetti et al, 1996).

Finally, phosphorylation, ubiquitinylation, palmoitolylation or interaction with membrane lipids are further mechanisms by which K^+ channels activity can be modulated.

Voltage-gated K^+ channels containing six transmembrane domains with one pore

The study of the structure of K^+ channels has given a great contribution to the understanding of the mechanisms underlying the functioning of voltage-gated ion channels. In particular, X-ray crystallography studies on procariotic and mammalian K^+ channels have clarified the molecular features that determine the selectivity filter, the VSD, and the conformational changes that mediate the channel gating (MacKinnon, 2004). In particular, in these studies the pore has been individuated in a hydrophobic aminoacids-rich cavity of about 10 Å-diameter, followed by a 12 Å-long region, that represent the selectivity filter; in the latter region, a conserved aminoacid motif (TVGYG) is present. According to this model, the hydrophobic region pushes hydrated K^+ ions to the selectivity filter, where the aminoacids of the conserved motif substitute water molecules in the interaction with K^+ ions, thus permitting the rapid flow of the

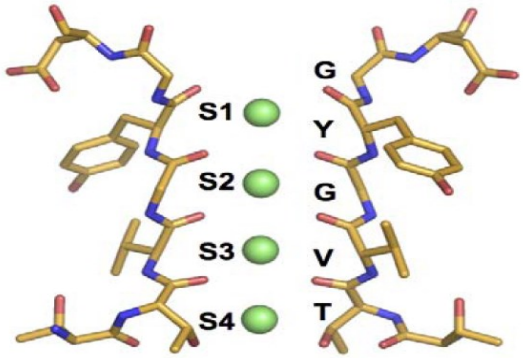

Figure 2. Molecular structure of procariotic KcsA potassium channel. The interaction of K^+ ions (in green) with aminoacidic sequence T-V-G-Y-G is also shown (modified from Lockless et al, 2007. PLoS Biol 5(5):e121).

cations along the cavity (Long et al, 2005 a-b). X-ray crystallography has also clarified the conformational changes occurring in the VSD, whose function had been investigated in many studies by using different techniques ("gating" current measurements, Armstrong and Bezanilla, 1974; mutagenesis studies, Papazian et al, 1991, Perozo et al, 1994; fluorescence studies, Mannuzzu et al, 1996, Cha and Bezanilla, 1997). In these studies, S4 segment was indicated as the main determinant of voltage-sensitivity, due to the presence of several positively-charged aminoacids (lysine or arginine), able to sense the variations in membrane potential and trigger the conformational changes of the protein leading to channel opening. Positively-charged aminoacid in S4 segment can interact with different negatively-charged residues in the S1-S3 region; these interactions seem to be very important for both channel stabilization and gating charge movements (Miceli et al., 2011). Movements of S4 segment are supposed to be translated to pore opening through a mechanism involving S4–S5 linker. Indeed, it has been proposed that, upon membrane depolarization, S4 outward movement, by pulling onto the S4–S5 linker, causes the bending of the S6 gating hinge to open the S6 intracellular helix bundle, leading to pore opening (Long et al., 2005a and b). However, the exact rearrangements occurring in the VSD are not fully understood, and at least three different models have been proposed (Miceli et al., 2011):

- *The helical screw or sliding helix model* propose that, when the membrane is depolarized, the S4 helix rotates along its length and translate along its axis, thus moving outwardly by a length corresponding to about three α-helical turns. The outward movement involves the sequential interaction between positively-charged and negatively-charged residues during VSD activation.
- *The transporter model* suggests that, during activation S4 would mainly undergo rotational movements without significant translational movements; upon membrane depolarization, arginines in the S4 segment would move from a crevice in contact with the intracellular solution into another crevice in contact with the extracellular solution. The resting and activated positions of the VSD would be stabilized by ionized

hydrogen bonds between the S4 arginines and two negatively charged clusters located in the S1, S2 and S3 helices.

- *The paddle model* proposes that S4 and part of S3 form a helical hairpin, or paddle, that freely moves by a large extent (15–20 Å) across the lipidic bilayer during each gating cycle; this large movement would be transmitted to the pore region through the S4-S5 linker, thus causing the pore opening. However, paddle model seems to be incompatible with several experimental evidence obtained in other K_v; since this model is mainly based on the crystal structure of the bacterial channel KvAP (Jiang et al., 2003a and b) it has been proposed that this model is based on a non native state of the channel caused by artifacts of the crystallization procedure (Catterall, 2010).

As stated before, voltage-gated K^+ channels are formed by six hydrophobic segments spanning the membrane, named S1-S6. The pore region is formed by S5-S6 domains, while S1-S4 segments represent voltage-sensing domain (VSD).

Functional K^+ channels are formed by the assembly of four α-subunits, both in homomeric or in heteromeric configuration. Protein region responsible for tetramerization are located in the N-terminus (K_v1, Li et al., 1992; Shaker, Shao and Papazian, 1993) or in the C-terminus (K_v10, K_v11 e K_v7; Ludwig et al, 1997; Kupershmidt et al, 1998; Schwake et al, 2000) of α-subunits.

The K_v7 channel family

The family of voltage-dependent K_v7 (KCNQ) K^+ channel comprises five members, namely $K_v7.1$-$K_v7.5$, each showing a distinct tissue distribution (Soldovieri et al., 2011). As other K_v channels, K_v7 channels are composed by six transmembrane domains (named S1-S6), a short N-terminal and a longer C-terminus, both located in the cytoplasmic side. Channel pore is formed by S5-S6 domains, while transmembrane regions S1-S4 constitute the voltage sensing domain (VSD), which allows channel gating in response to changes in membrane potential. In particular, S4 segment contains from four to six positively charged arginines separated by two to three uncharged residues; unlike other K_v channels, the third R is replaced by a neutral glutamine residue.

The long C-terminus is a typical feature of K_v7 channels and it is organized in four α helices (named A-D) containing different sites responsible for heteromeric and homomeric assembly, interaction with regulatory molecules, subcellular localization, and binding of accessory proteins (Haitin e Attali, 2008). Among them we can recognize:

- *Calmodulin*. The regulatory protein calmodulin (CaM) seems to be constitutively bound to the COOH-terminal region of $K_v7.2/3$ channels, irrespective of the intracellular Ca^{2+} concentration ($[Ca2]_i$), in particular to two sequences in helices A and B. Calmodulin effects on K_v7 channel have not been elucidated yet. In general, CaM is believed to play a key role for K_v7 channel folding and trafficking (Wen e Levitan, 2002; Yus-Najera et al, 2002; Gamper e Shapiro, 2003), but also in regulating K_v7 currents in response to changes in intracellular Ca^{2+} levels.
- *Syntaxin 1A*. Helix-A seems to mediate $K_v7.2$ channel interaction with the plasma membrane protein syntaxin 1A, thus addressing this subunit to pre-synaptic sites in neurons (Regev et al., 2009)
- *Phosphatidylinositol-(4,5)-Bisphosphate (PIP2)*. This lipid seems to stabilize the open state of K_v7 channels (Delmas and Brown, 2005). Indeed, differences in the single channel open probability among K_v7 channels subunits appear to be dependent on their intrinsic affinities for intracellular PIP2 (Li et al., 2005). The binding site for PIP2 is still unknown, although recent evidence suggest as possible binding site a region between helices A and B (Hernandez et al., 2009).
- *Kinases.* C-terminal region contains phosphorylation sites for different kinases such as PKA and PKC, which interact with anchoring protein AKAP 79/150 in a trimeric complex (Hoshi et al, 2003); in addition, tyrosin-kinase Src (Gamper et al, 2003) can suppress channel activity. Putative phosphrylation sites have been individuated for other protein such as EGF (Jia et al, 2007).
- *Ankyrin G*. An interaction domain for the adaptor protein Ankyrin-G has been identified in Kv7.2 and Kv7.3, but not for other Kv7 subunits. This "adaptor" protein mediate heteromeric Kv7.2/3 channels localization at

the axonal initial segment and Ranvier nodes (Pan et al, 2006; Rasmussen et al, 2007).

- *Subunit Interaction Domain*. Multimerization domains and subunit-specific heteromerization have been identified in the helices C and D (Schwake et al., 2003). In particular, a coiled-coil structure composed by the assembly of four parallel helices has been identified in $K_v7.4$ subunit by crystallography studies (Howard et al., 2007). However, additional sites for multimerization have been suggested for other region of the protein (Lundby et al., 2010).

- *Nedd4–2*. A binding motif for the ubiquitin-protein ligase Nedd4–2 has been found in C-terminal of $K_v7.1$. Nedd4-2 negatively regulates currents elicited by $K_v7.2/3$, $K_v7.3/5$ channels and $K_v7.1$/KCNE1 heteromultimers, possibly by promoting internalization and degradation of these complex (Jespersen et al., 2005; Ekberg et al., 2007).

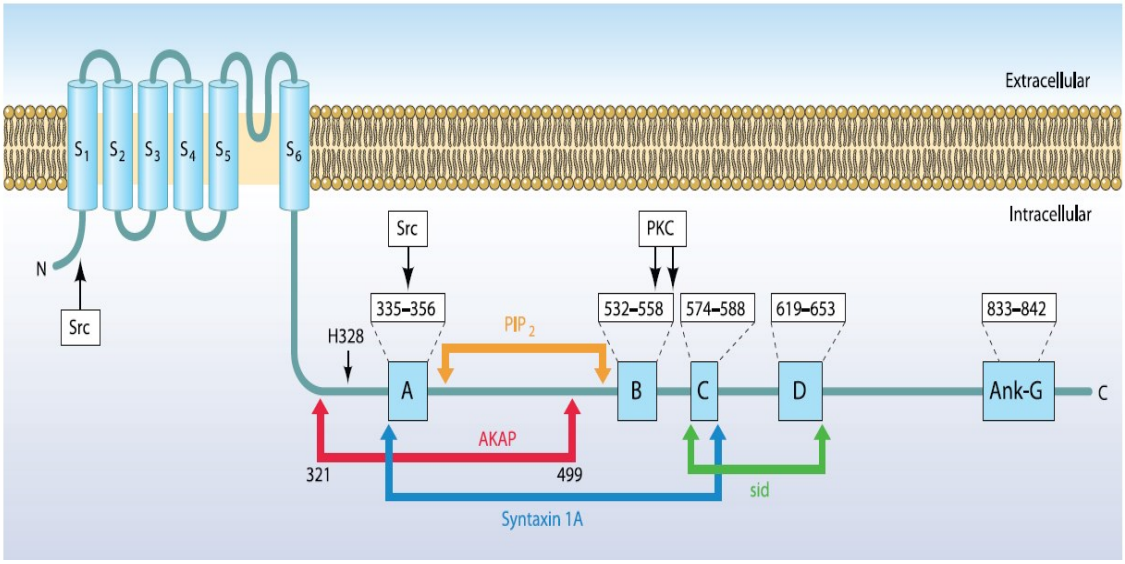

Figure 3. Schematic representation of C-terminal region of K_v7 subunits (From Soldovieri et al., 2011)

As stated before, each K_v7 subunit shows a distinct tissutal expression pattern. A first distinction can be made between $K_v7.1$, that is mainly expressed in the heart (but also in epithelia and inner ear) and do not associate with other members of the family, and $K_v7.2$- $K_v7.5$, that are often referred to as "neural"

K_v7 channels, for their wide distribution in the nervous system (Brown and Passmore, 2009). In particular, $K_v7.2$ and $K_v7.3$ (often in heteromeric conformation) are expressed in both peripheral and central neurons, $K_v7.4$ is present in the inner ear and in neurons of acoustic pathway, while $K_v7.5$ is expressed in several brain regions and in sympathetic ganglia. Nevertheless, more recent evidence have demonstrated that K_v7 channels are expressed in many other tissues, such as visceral and vascular smooth muscle (Jepps et al., 2013), and skeletal muscle (Iannotti et al., 2010), where they regulate muscular tone and differentiation/response to injury, respectively.

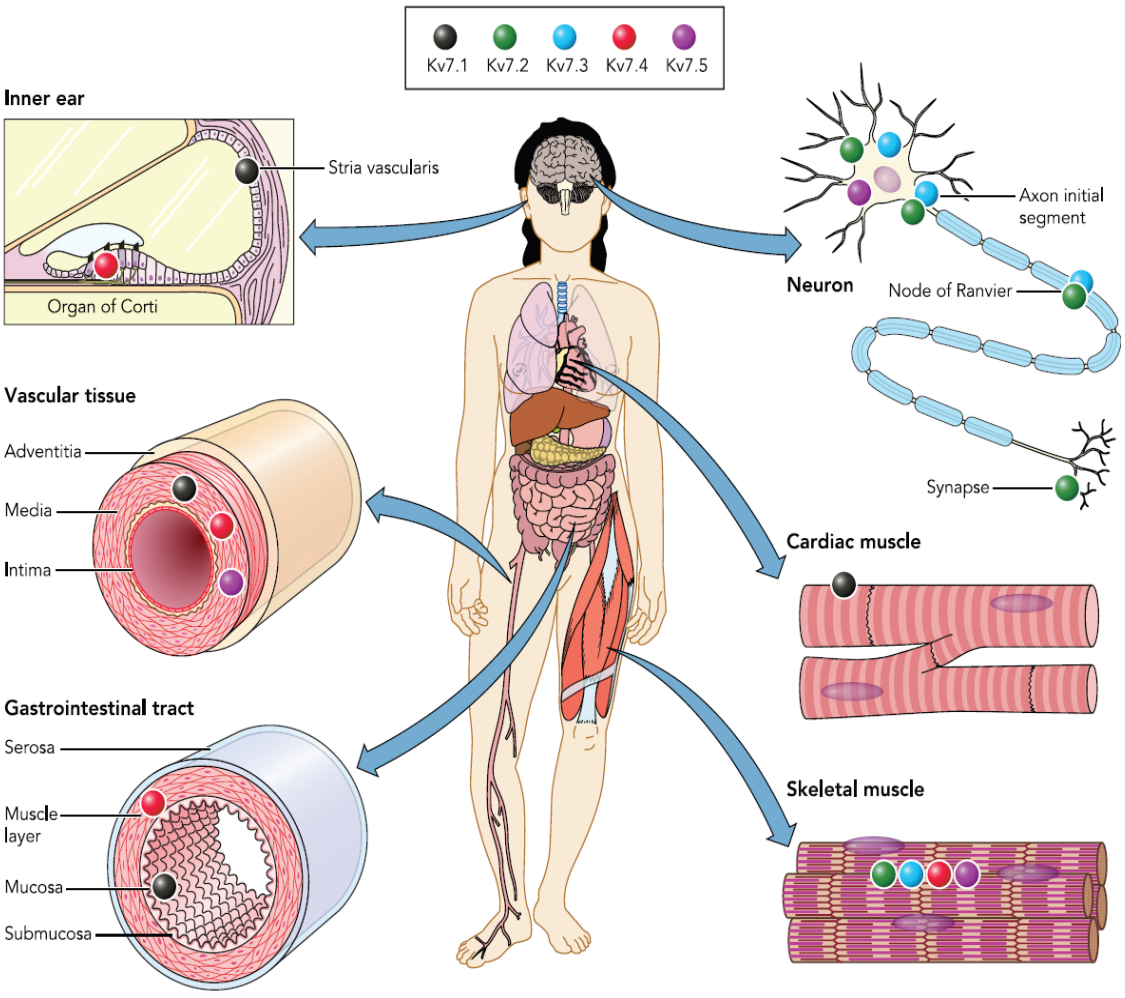

Figure 4. Tissutal distribution of K_v7 subunits (from Soldovieri et al., 2011)

K_v7 channels underlie K^+ conductances which repolarize cells, thus reducing excitability. In particular, cardiac $K_v7.1$ subunits, in association with KCNEs

subunits, mediates an important K^+ current, called I_{KS} that is a major component of the delayed rectifier current activated in the repolarization phase of cardiac cylce (Sanguinetti et al., 1996). By contrast, "neural" K_v7 channels do assembly in homo- or hetero-tetramers to underlie M-current (I_{KM}: Brown and Adams, 1980), a repolarizing current that reduce neuronal excitability especially after prolonged stimuli; this phenomenon is known as "spike frequency adaptation". M-current is regulated by several $G_{q/11}$-coupled receptors such as muscarinic receptors (hence its name), but also adrenergic-, angiotensin II-, substance P- and bradykynin- receptor. Activation of these receptors does suppress I_{KM} mainly by PLC-mediated reduction of PIP2 levels, which stabilize open conformation of the channel. Physiological relevance of M-current has been demonstrated at a somato-dendritic and axonal level, where it participates in the integration of post-synaptic inputs (Cooper et al, 2001), as well as at Ranvier's node (Devaux et al, 2004). Moreover, M-current is expressed also pre-sinaptically, where it modulates neurotransmitters release (Martire et al., 2004). Given their relevance in regulating such delicate processes, genetic alteration of K_v7 subunits are often associated to inherited diseases.

K_v7 subunits and genetic diseases

$K_v7.1$. kcnq1 gene, encoding for $K_v7.1$ subunit was cloned in 1996 (Wang et al 1996), as associated to Long QT Syndrome (LQTS), a pathologic condition characterized by a longer QT interval at the electrocardiogram (ECG) and thus predisposing to severe and possibly lethal arryhitmias such as torsades de pointes and consequent ventricular fibrillation. Several mutations have been found in kcnq1 gene, most of them impairing protein trafficking, interaction with regulatory molecules such as PIP2, or channel function (loss of function mutations). Such genetic alterations can be inherited as dominant (Romano-Ward syndrome) or in recessive form (Jervell and Lange-Nielsen syndrome); in the latter case, given the expression of $K_v7.1$ in the inner ear, bilateral deafness accompanies the severe cardiac dysfunction. Interestingly, also mutations enhancing the activity of $K_v7.1$ channel (gain of function alterations) have been

found; they are responsible of short QT syndrome, characterized by ECG T-wave alterations, increased risk of atrial fibrillation and sudden infantile or adult death syndrome (SIDS/SADS) (Hedley et al, 2009).

K_v7.1 has gained attention as a possible antiarrhythmic pharmacological target; moreover, given its expression in gastrointestinal epithelia, drugs modulating K_v7.1-mediated currents might be interesting tools in the treatment of fluid transport dysfunction.

K_v7.2 and K_v7.3. Genes encoding for K_v7.2 and K_v7.3 (named kcnq2 and kcnq3) have been cloned in 1998 because of their association to a rare hereditary epilepsy of the newborn, called Benign Familial Neonatal Seizures (BFNS) (Singh et al, 1998; Charlier et al, 1998; Bievert et al, 1998). K_v7.2 and K_v7.3 show a distribution largely overlapping in different areas of the central nervous system, as well as in peripheral neurons. More recently, their expression has been detected also in the cochlea, in the spiral ganglion and in sensory neurons of the carotid body. K_v7.2 and K_v7.3 are the main molecular determinants of M-current (I_{KM}), a slowly activating/deactivating and non-inactivating repolarizing current that can be suppressed by the activation of muscarinic receptors. BFNS-causing mutations hit more often kcnq2 gene than kcnq3 (10:1 ratio); while known K_v7.3 mutations are missense, K_v7.2 mutations are various, such as truncations, splice site defects, missense, non-sense, frame-shift mutations, as well as sub-microscopic deletions or duplications; moreover, many of them impair C-terminal region of the protein (Soldovieri et al., 2011). More recently, mutations in kcnq2 have been associated to other neurological disorders, such as Peripheral Nerve Hyperexcitability (Dedek et al, 2001; Wuttke et al, 2007).

K_v7.4. The product of kcnq4 gene is distributed in the inner ear and in neurons of acoustic pathway; expression in other brain areas seems to be low, although it has been recently demonstrated its presence on dopaminergic neurons of meso-limbic and nigro-striatal pathway (Hansen et al., 2006). Moreover, K_v7.4 is highly expressed in non-neuronal tissues, in particular in smooth and skeletal muscle, and variations in its levels seem to be correlated to pathophysiological processes such as hypertension and differentiation (Jepps et al, 2011; Iannotti et

al., 2013). Given its wide expression in the inner ear, it is not surprising that mutations in $K_v7.4$ are associated to an hereditary, non-syndromic, progressive form of sensorineural hearing loss called DFNA2 (Kubisch et al., 1999). Most DFNA2-causing mutations in $K_v7.4$ are missense alterations affecting amino acids located within or close to the channel pore or C–terminal region and causing hearing loss via a dominant-negative effect, often with a severe phenotype; deletions, which cause DFNA2 via haploinsufficiency, and are assocated to a later-onset of symptoms compared to missense mutations (Smith and Hildebrand, 2008).

$K_v7.5$. Last K_v7 channel to be cloned, kcnq5 gene products are expressed in nervous system and they largely overlap $K_v7.2$ and $K_v7.3$ distribution, thus suggesting that it does contribute to the molecular heterogeneity of M-current. In particular, $K_v7.5$ do assemble with $K_v7.3$ and $K_v7.4$ but not with $K_v7.2$; it has been proposed that $K_v7.5$ expression in heteromeric channels is a way to reduce M-current, possibly by "sequestering" $K_v7.3$ subunits available to form the more "efficient" Kv7.2/Kv7.3 heteromers, known to underlie larger currents. As for other K_v7 channels, $K_v7.5$ expression has been individuated also in non-neuronal tissues, such as smooth and skeletal muscle (Jepps et al., 2011; Iannotti et al., 2010).

BFNS

Mutations in $K_v7.2$ and $K_v7.3$ are associated to Benign Familial Neonatal Convulsions (BFNS), a neonatal form of epilepsy characterized by an early age of onset (day 3) and by the spontaneous disappearing of symptoms between the first and the sixth to 12th month of life. BFNS phenotype is characterized by a wide spectrum of seizure types (tonic or apneic episodes, focal clonic activity, or autonomic changes), usually lasting one or two minutes; symptoms may be confined to one body part, migrate to other body regions, or generalize. Most patients develop normally, although about 10%-15% of individuals with BFNS may experience epileptic seizures later in life (Bellini et al., 2010). Haploinsufficiency seems to be a main pathogenetic mechanism, since reduction

of M-current density by only 25% is sufficient for the onset of BFNS. Several hypotheses have been made to explain the disappearance of seizures with brain development; among them, some concern I_{KM} and $K_v7.2$ subunits expression, while others focus on differences in inhibitory conductance in neonatal brain when compared to adult one. In particular, it has been suggested that fetal neurons express a shorter and non-functioning $K_v7.2$ splice variant (Smith et al., 2001), or that $K_v7.2$ subunits show a different subcellular distribution in adult neurons with respect to immature ones (Weber et al., 2006); moreover, it has been demonstrated that M-current density increases after the birth, thus contributes to disappearance of recurrent synchronous bursts characteristic of early phases of hippocampal development (Safiulina et al, 2008). On the other hand, it is known that in immature brain, due to prevalent activity of the co-transporter Na^+-K^+-$2Cl^-$ (NKCC1), chloride gradient is inverted; therefore, activation of GABA receptors mediate cell-depolarization thus giving an excitatory stimulus rather than inhibit neurotransmission (Okada et al, 2003). As a consequence, neonatal brain might be more sensible to M-current dysfunction, thus leading to epilepsy that disappears in adulthood.

Despite the common "benign" phenotype associated to mutations in $K_v7.2$ and $K_v7.3$, several recent studies have described kcnq2 gene alterations in neonates affected by more severe neurological disorders known as $K_v7.2$ related neonatal epileptic encephalopathy (kcnq2-NEE), such as pharmacoresistant seizures with psychomotor retardation (Nabbout and Dulac, 2011), neuroradiological alterations (mostly affecting basal ganglia and thalamus), as well as Ohtahara syndrome, an early-onset age-related epileptic encephalopathy characterized by typical suppression-burst EEG pattern within the first months of life and poor outcome in terms of psychomotor development and seizure control (Bellini et al., 2010). The reasons of such a wide spectrum of phenotypes caused by mutation in the same gene are not completely understood; differences in the type of mutations as well as protein-region affected, and their functional consequences on channel expression and/or activity is a possible explanation.

Animal models for K_v7 channels-associated diseases

Pahophysiological role of M-current has been evaluated in different animal models that reproduced the loss of K_v7 subunits by deleting gene expression (knock-out mouse) or by the introduction in the genome of modified channels with dominant-negative effects (transgenic mice). Among them we can mention:

- **$K_v7.2$- $K_v7.3$**. Two animal models for BFNS have been obtained by the introduction in $K_v7.2$ and $K_v7.3$ genes of two human BFNS-causing mutations in two different mice-strains, to better understand also the possible interference of genetic background (Singh et al, 2008). The mutations (A306T in $K_v7.2$ e A311V in $K_v7.3$) affected pore-region, thus causing a dramatic decrease of channel activity. Homozygous mice for $K_v7.2$-A306T or $K_v7.3$- A311V showed early onset spontaneous generalized tonic-clonic seizures, with electro-encephalographic alteration suggesting a lymbic origin of convulsions. Moreover, adult homozygous mice had recurrent seizures that triggered molecular plasticity including ectopic neuropeptide Y (NPY) expression; in addition, overall mortality was increased when compared to control littermate, with differences depending on mutation and murine strain. Interestingly, despite the severe phenotype, no significant morphological alteration, such as hippocampal mossy fibers sprouting or neuronal loss, was found in homozygous mice, thus paralleling the normal neurodevelopmental cognitive profile exhibited by most BFNS patients (Singh et al., 2008).
- **$K_v7.4$.** Two animal models of $K_v7.4$ function knock-down are available: a knock-out ($Kv7.4^{-/-}$) and a transgenic mouse in which a DFNA2-causing mutation exerting dominant negative effects on wild-type $K_v7.4$ has been introduced ($K_v7.4^{dn/dn}$) (Kharkovets et al, 2006). Both mice display an apparent normal phenotype in early phases, while hearing function is progressively impaired later in life, due to death of cochlear outer hair cells, where $K_v7.4$ expression seems to be particularly abundant; this phenotype reproduce the progressive sensorineural hearing loss showed by DFNA2 patients. It has been suggested that cell death is a consequence of chronic depolarization determined by lack of $K_v7.4$-mediated currents.

- **K_v7.5.** A transgenic mouse carrying a mutation in K_v7.5 (similar to the one in K_v7.4 used to generate $K_v7.4^{dn/dn}$ mouse model) exerting dominant negative effects has been recently generated (Tzingounis et al, 2010). Such mouse showed no apparent clinically-relevant phenotype and normal brain morphology; however, in the CA3 area of hippocampus, a region that highly expresses K_v7.5 channels, a decrease in the medium and slow afterhyperpolarization currents was observed.

Drugs acting on K_v7 channels

Given the rising interest in M-channels pathophysiology and related possible therapeutic opportunities, a number of compounds acting on K_v7 subunits have been developed throughout years. Moreover, although some of them are not in clinical use, K_v7 activators and blockers do represent a valid tool to further understand M-current role.

Blockers. Linopiridine is one of the first molecules identified as K_v7-blockers. Since it increases release of different neurotransmitters, such as acetylcholine, serotonin, dopamine and glutamate in different animal models, linopiridine has been proposed as a cognition enhancer. Nonetheless, clinical trials investigating its efficacy in diseases characterized by cognitive impairment such as Alzheimer's Disease failed to demonstrate symptoms improvement, possibly because of its low potency on K_v7 channels as well as a negative pharmacokinetic profile with consequent cholinergic side effects. Linopiridine analogues such as XE-991 have been developed with the aim to overcome such issues; however, their use is still restricted to pre-clinical phases (Wulff et al., 2009).

Activators. Flupirtine is a triaminopyridine successfully used in clinical practice in some European countries since 1984 for its centrally acting, nonopioid analgesic properties, but without notable anti-inflammatory and antipyretic activity. It is also provided with muscle relaxant actions, thus suggesting its use in muscular pathology such as fibromyalgia. Later, flupirtine was shown to have also antioxidant, neuroprotective and anticonvulsant activity, although at doses

higher than those producing analgesia. Structure-activity optimization of flupirtine yielded retigabine (chemical name N-(2-amino-4-(4-fluorobenzylamino)-phenyl)-carbamic acid ethyl ester), the prototype I_{KM} opener. Retigabine displayed more effective anticonvulsant activity when compared to flupirtine, being active in nearly every animal seizure model, with an overall profile different from any other known drug (Porter et al., 2007). In addition to the activation of K_v7-mediated current, retigabine also potentiates $GABA_A$-mediated currents at concentrations at least 10–30 times higher than those effective on M-current; a weak blocking action on ligand- (kainate and NMDA receptors) and voltage-gated (sodium and calcium) channels were also observed (Rundfeldt, 1997 and 1999). As flupirtine, retigabine exerts antioxidant activity in vitro (Boscia et al., 2006; Gassen et al., 1998), a pharmacological property which might explain at least in part the neuroprotective effects shown by this compounds. Retigabine increases I_{KM} by determining an hyperpolarizing shift in the voltage-dependence of the channel activation process and an increase in the maximal opening probability of these channels; although the size of these effects is different depending on channel subunits composition (higher in $K_v7.2$ and $K_v7.3$ homo- and hetero-mers, lower for $K_v7.4$ and $K_v7.5$), retigabine is considered a non-selective K_v7 activator. Noticeably, retigabine does not activate cardiac $K_v7.1$ channels. By contrast, a higher subunit-selectivity is a characteristic of ICA-27243, a compound belonging to the chemical class of substituted benzamides. ICA-27243 has also anticonvulsant properties, as demonstrated by studies in preclinical models of seizures (Wickenden et al., 2008), and preferentially activates current elicited by $K_v7.2/K_v7.3$ heterotetramers, while its potency on $K_v7.4$ or $K_v7.3/K_v7.5$ channels is 20-fold and-100-fold lower, respectively (Roeloff et al., 2000). Other molecules provided with agonistic activity on K_v7 channels are zinc pyrithione (Xiong et al., 2007), which potentiates K^+ currents elicited both by cardiac Kv7.1 and neural $K_v7.2$-5 subunits, except those sustained by $K_v7.3$ channels, BMS-204352, originally developed as an opener of BK_{Ca} channels (Korsgaard et al., 2005), and the acrylamide compound, (S)-1 (Bentzen et al, 2006), both displaying a stronger action on channels formed by $K_v7.4$ subunits, and NS15370, a more potent retigabine-analogue able to activate all K_v7 subunits at

sub-micromolar concentrations (Dalby-Brown et al., 2013). Interestingly, commonly used drug as diclofenac can also activate M-current. In particular, it has been demonstrated that diclofenac-derivatives with poor or absent cyclooxygenase-blocking activity reduced neuronal excitability and/or showed anticonvulsant effects in murine models of seizures (Peretz et al., 2007 a and b).

A better understanding of the differential subunit selectivity of K_v7 activators has been achieved by studies on drug-binding sites. For instance it has been suggested that retigabine binds to a hydrophobic pocket located between the cytoplasmic parts of the S5 and the S6 transmembrane domains in the open channel configuration, where a tryptophan residue in the intracellular end of the S5 helix (W236 in the $K_v7.2$ sequence) seems to play a crucial role (Wuttke et al., 2005; Schenzer et al., 2005). Indeed, replacement of this residue with a smaller and less hydrophobic amino acid (leucine) largely impeded the ability of retigabine to increase M-current. Additional aminoacids (in $K_v7.2$ sequence: Leu243 in S5, Leu275 within the inner pore loop, Gly301 in the S6 segment, and Leu299 in S6 of the neighboring subunit) seem also to be involved in the formation of the complete retigabine binding site (Lange et al., 2009); interestingly, except for Leu275, these amino acids are conserved among all neural K_v7 subunits but are missing in the $K_v7.1$ subunit primary sequence, thus possibly explaining the lack of effect of retigabine on $K_v7.1$ subunits. The tryptophan in the S5 segment seems also to be important for the binding of other I_{KM} activators, such as S-(1) and BMS-204352, while zinc pyrithione, are supposed to bind to a different aminoacid sequence in the pore. These observations might explain the additive effects on I_{KM} exerted by retigabine and zinc pyrithione (Xiong et al., 2008). By contrast, diclofenac and its derivatives binding site seems to be in close proximity to the external surface of the voltage-sensing domain, at the interface of helices S1, S2, and S4. Indeed, these compounds are still able to potentiate the K^+ currents elicited by the $K_v7.2$ W236L mutant. Similar to these drugs, the selective $K_v7.2/K_v7.3$ opener ICA-27243 was also found to bind to the voltage-sensing domain; the primary sequence of the region involved in ICA-27243 binding appears extremely

variable among Kv7 subfamily members, allowing the drug to selectively affect channels formed by specific Kv7 subunits.

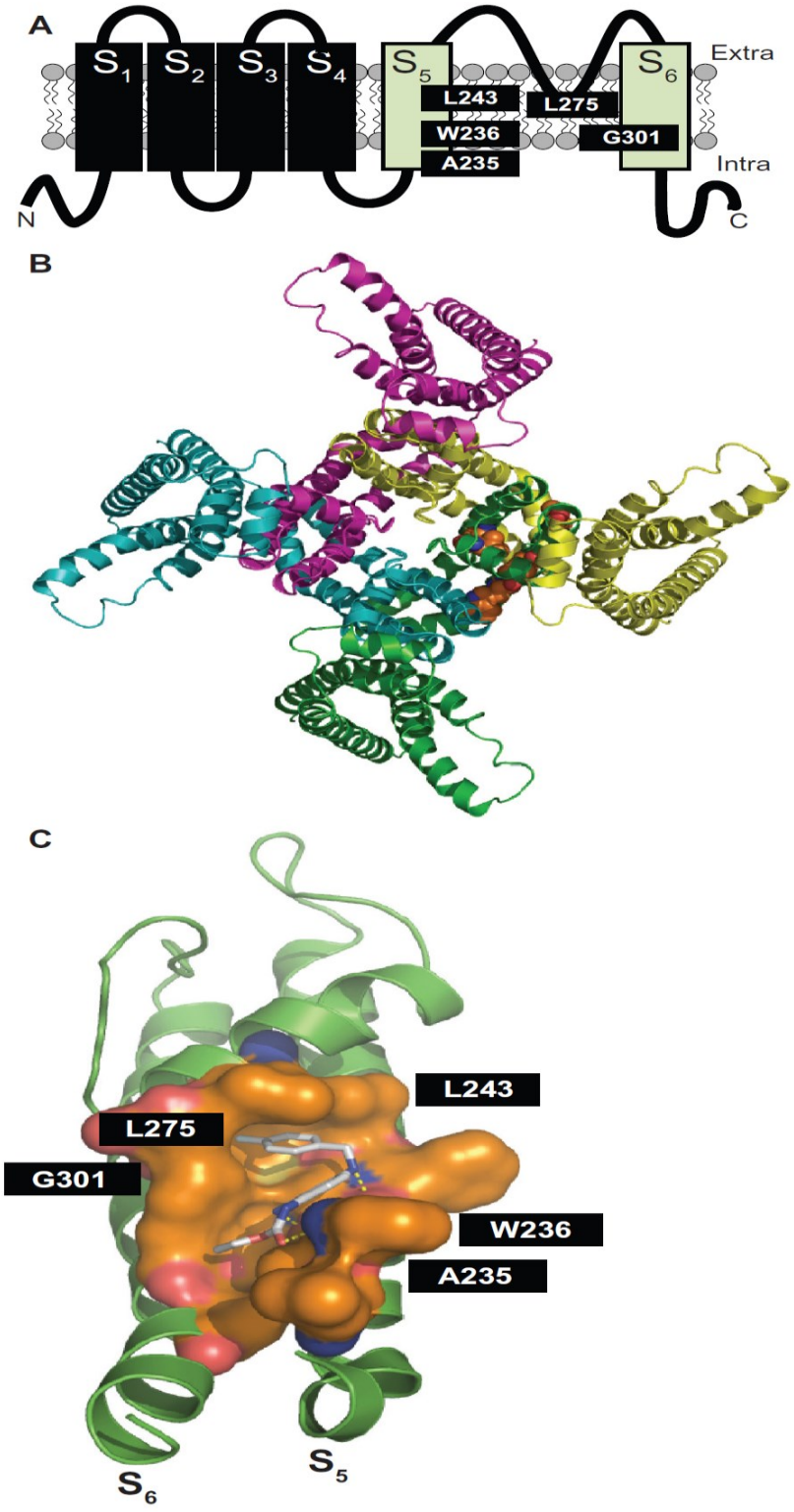

Figure 5. (A) Schematic topology of a single Kv7.2 subunit, with amino acids involved in retigabine binding are indicated. (B) top view of the overall structure of the channel formed by four identical Kv7.2 subunits, with one retigabine molecule bound. (C) enlarged view of the

retigabine binding site with the retigabine molecule docked into the channel cavity. From Barrese et al., Clin Pharmacol. 2010. 2:225-36)

K_v7 channels and neurodegeneration

The role of K_v7 channels in the regulation of cell death/survival, or protection from damage in neurons, in particular in the hippocampus, has been investigated in various experimental studies. Such studies do not clearly establish a neuroprotective or neurodegenerative role for K_v7 channels, probably because of the different experimental models used.

Indeed, it has been recently demonstrated that the activation of $K_v7.2/K_v7.3$ channels induced by the non-specific oxidant NEM could induce death in hippocampal primary neuronal culture, through the activation of the apoptotic pathway; this effect was reverted by the K_v7-selective blocker XE-991 or by exposure to high extracellular potassium concentration (Zhou et al., 2011).

On the other hand, other studies have pointed out the neuroprotective effects of I_{KM}-activators in different experimental models, such as hippocampal organotypic slice cultures (OHSCs) treated with NMDA or undergoing serum deprivation (Boscia et al., 2006), although in these models the neuroprotective effects of retigabine seem to be due to a non-specific anti-oxidant action more than a direct activation of M-current. According to this study, neuroprotective effects of flupirtine and retigabine are more noticeable in some hippocampal areas such as dentate gyrus, a brain region showing remodelling after chronic epileptogenic stimuli. Similarly, Gamper and collaborators (2006) demonstrated that exposure to retigabine reduced oxygen glucose deprivation (OGD)-induced death of OHSCs.

Flupirtine- and retigabine-induced neuroprotection has also been observed in two “in vivo” preclinical models of ischemia, namely the four vessels occlusion (4-VO) rat (Block et al, 1997) and a mouse model of cerebral photo-induced thrombosis (Bierbower et al, 2011); in both animal models, these drugs reduced infarct area and/or the subsequent cognitive impairment.

RATIONALE AND AIM OF THE STUDY

Many neuronal diseases are characterized by hyper-excitability. For instance, ischaemic stroke causes the activation of multiple processes, including ionic imbalance, increase in the extracellular concentration of glutamate and activation of the NMDA receptors, with following increase in intracellular calcium and cell death, peri-infarct depolarization (Doyle et al., 2008); epilepsy shows similar pathogenetic mechanisms (Costa et al., 2006). Excessive neurotransmitter release is a key events in the propagation of neuronal damage, and subsequent death, following ischaemia. Although glutamate release (and in particular on NMDA receptor over-stimulation) has been viewed as a main cause of neuronal damage, massive release of monoamine neurotransmitter such as dopamine, also occurs immediately following the onset of ischemia (Sarna et al., 1990). In particular DA levels achieved immediately following the onset of ischemia have been shown to be neurotoxic and directly contribute to the resulting cell death (Lieb et al., 1995). Given their demonstrated role in regulating neurotransmitter release in different brain areas (Martire et al., 2004), K_v7 channels might be interesting target in counteracting the abnormal modification occurring in hyper-excitability pathology such as stroke.

The prominent role of K_v7 channels (in particular $K_v7.2$) in reducing neuronal excitability is underlined by inherited disease due to mutations in $K_v7.2$ and $K_v7.3$, Benign Familial Neonatal Seizures. Interestingly, several recent reports have described alterations in $K_v7.2$ gene also in patients with pharmacoresistant epilepsies with psychomotor retardation, as well as in cases of epileptic encephalopathy (Weckhuysen et al., 2011). The molecular basis of such variability is still unknown, although it has been proposed that specific alterations affecting distinct aminoacids or different regions of the channel could explain the onset of “benign” epileptic phenotype rather than a severe encephalopathy.

Based on these premises, the aim of this study has been to investigate:

- The potential neuroprotective role of K_v7 channels in an in vitro model of ischemia, such as brain slices undergoing oxygen- and glucose-

deprivation. In particular, we have investigated the effects of the pharmacological modulation of K_v7 channels on dopamine release and on brain damage in slices obtained from rat caudate, a region primarily involved in ischemic stroke.

- The possible molecular basis of the different phenotypes caused by mutation in $K_v7.2$. In particular we have investigated the effects on the channel function determined by two mutations affecting the same residue in the voltage sensing domain of $K_v7.2$, namely R6Q and R6W, responsible for a form of epileptic encephalopathy and BFNS, respectively.

MATERIALS AND METHODS

Animal and slices. Adult male Wistar rats mice (10–12 weeks old) were killed by cervical dislocation, and the vault of the skull was rapidly opened to expose the brain, while being frequently irrigated with ice cold maintenance artificial cerebrospinal fluid (aCSF, composition in mM): NaCl (126.0), KCl (2.0), KH_2PO_4 (1.4), $MgSO_4$ (2.0), $NaHCO_3$ (26.0), $CaCl_2$ (2.4), (+)-glucose (10.0), bubbled for at least 30 min with 95% O_2/5% CO_2. The brain was then removed and placed in ice cold maintenance aCSF until slicing (less than 5 min). The brain was dissected quickly and coronal slices (400 μm thick) at the level of the striatum were cut and maintened in aCSF continually bubbled with 95% O_2/5% CO_2. Once cut, slices were left to equilibrate for 1–4 h at room temperature (21±1 ◦C), to allow recovery from any trauma associated with slicing (Toner and Stamford, 1996).

Fast Cyclic Voltammetry (FCV). The FCV recording apparatus comprised a slice chamber (approx. 2 ml) which was suspended over a water chamber and heated via a thermostatically controlled circulating water bath (Grant, Cambridgeshire, UK) and continuously perfused with normal- or OGD- aCSF (2 mM glucose, bubbled with 95% N2/5% CO2), kept at a temperature of 32.ºC, with a flow rate of 100 mL/h. FCV microelectrode was placed into the dorsolateral caudate nucleus, at a depth of approximately 75 μm below the slice surface, using a micromanipulator under microscope guidance. DA levels in the dorsolateral caudate nucleus were measured continuously by FCV at carbon fibre microelectrodes (Stamford, 1990). The signal was also digitalized and recorded using Spike7 software (Molecular Devices, CA). An increase in the current signal at +600 mV, together with a corresponding reduction peak at −200 mV, were characteristic of DA detection in the caudate nucleus (Stamford, 1990).

Experimental protocol for oxygen- and glucose- deprivation. Slices were allowed to equilibrate in FCV slice chamber for 15 min, to assess that no spontaneous dopamine release occured. They were then incubate with normal aCSF containing DMSO (control) or drug (treated) for 15min; insults were determined by superfusion of brain slices with OGD-aCSF, containing DMSO

(control) or drug (treated). For qPCR, western blot and TTC staining experiments, slices were also exposed for 30 min to normal aCSF containing DMSO or drug after OGD-superfusion, to mimic reoxygenation.

FCV data analysis. Analysis of data was performed offline using Spike7. Perfusion with OGD-aCSF typically evoked a large increase in DA from the slice and four parameters were measured: (1) time to onset of DA release from the initiation of OGD superfusion (T[on]); (2) time taken to reach maximum DA release after the onset of release (T[peak]); (3) maximum extracellular DA concentration (DA[max]); and (4) mean rate of DA release (DA/T).

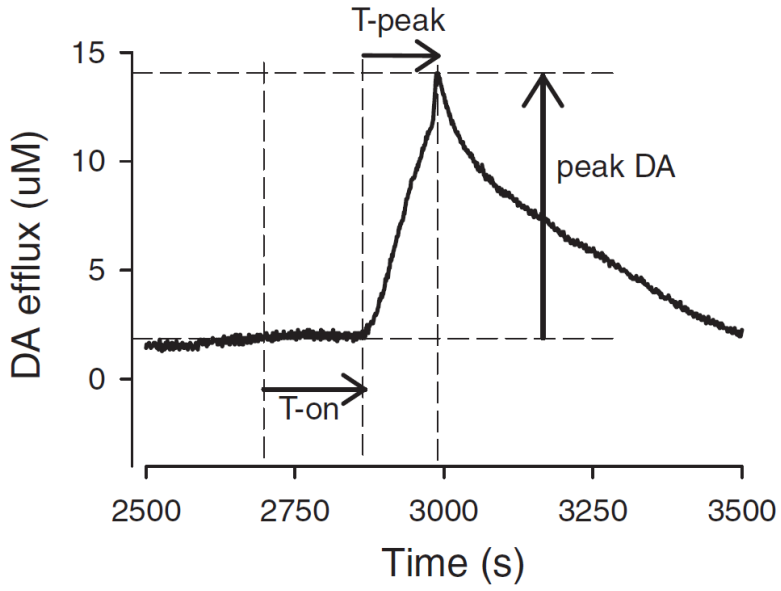

Figure 6. Variables recorded from voltammetry experiments. This figure is a close up from the dopamine release event brought on by OGD. See text for more information (from Davidson et al., 2011).

TTC staining. Slices were stained with 2,3,5-triphenyltetrazolium chloride (TTC) used at a dilution of 0.125% (w/v) in aCSF at room temperature in the dark for 30 min, then fixed in 4% paraformaldehyde solution; slices were photographed and analysed for percentage of caudate nucleus area stained, using ImageJ software (http://rsb.info.nih.gov/ij/).

Real time PCR. Total RNA was extracted from brain slices using the RNeasy Mini kit (Qiagen, U.K.) RNA was quantified using a Nanodrop Spectrophotometer (LabTech International) and reverse transcribed with Oligo (dT) primers and Moloney Murine Leukemia Virus (M-MLV; Invitrogen, U.K.).

Negative controls (RT-) were carried out in the absence of reverse transcriptase to check for genomic contamination. Quantitative mRNA analysis was determined using Precision-iC SYBR green master mix (PrimerDesign, Ltd., U.K.) with the CFX96 (Biorad, U.K.). Duplicate reactions were performed in 20µl volumes including 300nM primer mix (forward and reverse primer; PrimerDesign, Ltd., U.K.). Amplification protocol was as follow: 95°C for 10 min, 40 cycles of 95°C for 15 s, and 60°C for 1 min, during which time data was collected. Melt curve analysis, to ensure each primer set amplified a single product, completed the protocol and no template controls (NTCs) were run alongside all reactions to assess contamination. Cycle threshold (Ct) values were determined using Bio-Rad CFX96 software and the single threshold mode. Relative abundance of each gene of interest was calculated and normalised to the mean of gapdh housekeeping gene, using the $2^{-\Delta\Delta Ct}$ formula.

Western Blot. Brain slices were homogenized in 100 µL of lysis buffer (in mmol/L: 20 Tris base, 137 NaCl, 2 EDTA, 1% NP40, 10% glycerol, pH 8, and 10 µL/mL protease inhibitor cocktail; Sigma-Aldrich), incubated on ice for 30 minutes, centrifuged to remove cell debris, and denatured at 95°C for 5 minutes in the presence of sample buffer and reducing agent (Invitrogen). Samples were then loaded onto SDS-PAGE gels (4–12% Bis-Tris, Invitrogen), subjected to electrophoresis, and then transferred onto a polyvinylidene fluoride membrane (Amersham Biosciences). The membrane was then probed with an anti- Kv7.2 antibody (1:500; Millipore). Protein bands were visualized with enhanced chemiluminescence (Thermo Scientific) and hyperfilm (Amersham Bioscience). The membrane was then washed in PBS-Tween (0.1%) and subsequently reprobed for β-actin (1:5000; Sigma-Aldrich, A1978), used as loading control. Bands were quantified with Image J software.

Mutagenesis of K_v7.2 cDNA and Heterologous Expression of WT and Mutant KV7.2 cDNAs. Mutations were engineered in human K_v7.2 cDNA cloned into pcDNA3.1 by sequence overlap extension PCR with the Pfu DNA polymerase as described previously (Miceli et al., 2009). Briefly, mutations were introduced by amplifying, in three PCR reactions, a PmlI and HindIII cassette, subsequently cloned in pcDNA3.1 plasmid. Channel subunits were expressed in CHO cells by

transient transfection using Lipofectamine 2000 (Invitrogen) according to the manufacturer's protocol. A plasmid encoding for EGFP (Clontech) was used as transfection marker.

Whole-Cell Electrophysiology. Currents from CHO cells were recorded at room temperature (20–22 °C) 1 to 2 d after transfection by using an Axopatch 200A (Molecular Devices) and the whole-cell configuration of the patchclamp technique, with glass micropipettes of 3 to 5 MΩ resistance. The extracellular solution contained (in mM) 138 NaCl, 2 CaCl2, 5.4 KCl, 1 MgCl2, 10 glucose, and 10 Hepes, pH 7.4 adjusted with NaOH; the pipette (intracellular) solution contained (in mM) 140 KCl, 2 MgCl2, 10 EGTA, 10 Hepes, 5 Mg-ATP, pH 7.3 to 7.4 adjusted with KOH. pCLAMP software (version 10.0.2) was used for data acquisition and analysis. Currents were corrected offline for linear capacitance and leakage currents by using standard subtraction routines (Clampfit module of pClamp 10). To generate conductance–voltage curves, the cells were held at −80 mV, then depolarized for 1.5 s from −80 mV to +20/+120 mV in 10-mV increments, followed by an isopotential pulse at 0 mV of 300 ms duration. Current values at the beginning of the 0-mV pulse were measured, normalized, expressed as a function of the preceding voltages, and fitted to a Boltzmann distribution of the form y = max/[1 + exp(V1/2 − V)/k] to obtain V1/2 and slope factor k. Current traces were fit to a single- or a double-exponential function.

Computational Modeling. All simulations were carried out with the NEURON program, version 7, by using a previously described 3D model of a CA1 pyramidal neuron. Uniform passive properties were used over the entire neuron, with Cm of 0.75 μF/cm2 and Rm of 37.3 kΩ/cm2 (τm = 28 ms). Active somatic and dendritic properties included the following conductances: sodium (I_{Na}), potassium delayed rectifier (I_{DR}), potassium transient (I_A), potassium M (I_{KM}), and nonselective, hyperpolarization-activated (I_h); a low-threshold Ca^{2+} and a Ca^{2+}-dependent K^+ conductance, as well as a simple Ca^{2+} extrusion mechanism, were also included. I_{Na}, I_{DR}, Ca^{2+}-, and Ca^{2+}-dependent K^+ conductances were included at uniform density over the somatodendritic region, and I_A and I_h linearly increasing with distance from the soma. The I_{KM}

properties were implemented to fit the steady-state and kinetic values obtained in this work.

RESULTS

In previous studies conducted by our research group, it was demonstrated that pharmacological modulation of M-current modified neurotransmitters release in different brain areas (Martire et al., 2004). In particular, K_v7 activator retigabine was able to decrease dopamine release in striatal synaptosomes exposed to high extracellular K^+ concentrations. Effects of retigabine were concentration-dependent, with an IC_{50} of about 0.5 μM (Martire et al., 2007).

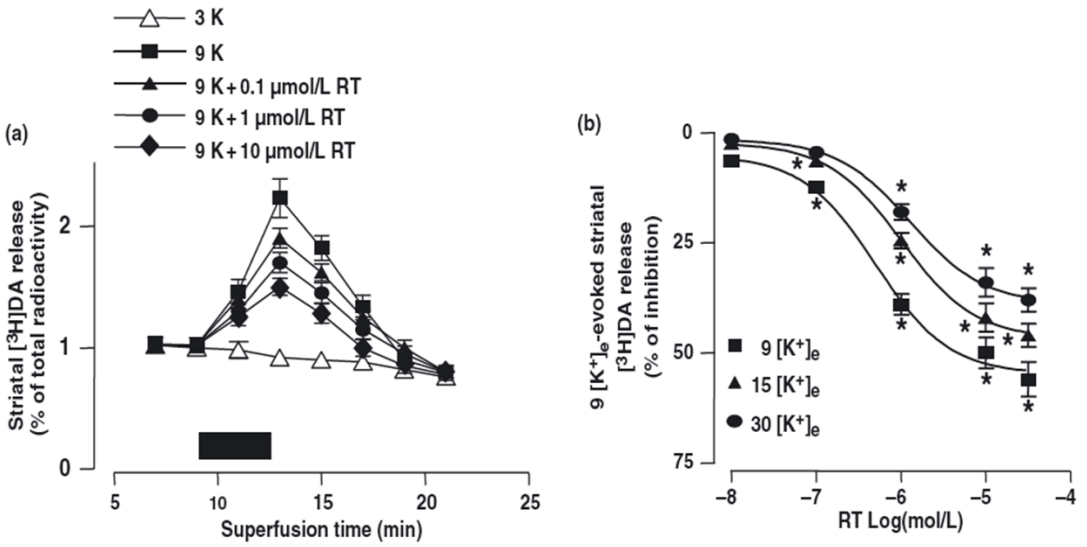

Figure 7. Effects of retigabine on high extracellular K^+-evoked dopamine release on rat striatal synaptosomes. From Martire et al., 2007

Since striatum is a brain area often damaged in most cases of ischemic stroke, and given that massive dopamine release occurs during ischemia, reaching neurotoxic levels and contributing to the propagatation of brain damage (Lieb et al., 2010), we investigated the potential role of K_v7 channels in modulating brain damage induced by anoxia in the striatum, using brain slices undergoing oxygen- and glucose- deprivation (OGD) as an experimental model of ischemia. This in vitro model confers some advantages such as the possibility to control the chemical environment and the temperature, factors which both affect neurological outcome following OGD or the avoidance of the use of anaesthetics, which are known to affect neurotransmitter function and can be neuroprotective. Dopamine release was measured by means of Fast scan Cyclic Voltammetry (FCV), an electrochemical technique that can be used to monitor

release of endogenous monoamines levels because of their property to be oxidized at low voltages. In particular, a triangular-shape voltage that is sufficient to oxidize dopamine is applied to a carbon fiber microelectrode; dopamine is oxidized to form dopamine-o-quinone which is reduced back to dopamine. During this redox reaction electrons are transferred between molecules and the microelectrode (electrolysis), thus producing a current flow at the electrode surface that is directly proportional to dopamine molecules present in the fluid. If current are plotted against the applied potential, it is possible to obtain a cyclic voltammogram, which is unique for each substance and allows to recognize the molecular identity of the molecule (John and Jones, 2007).

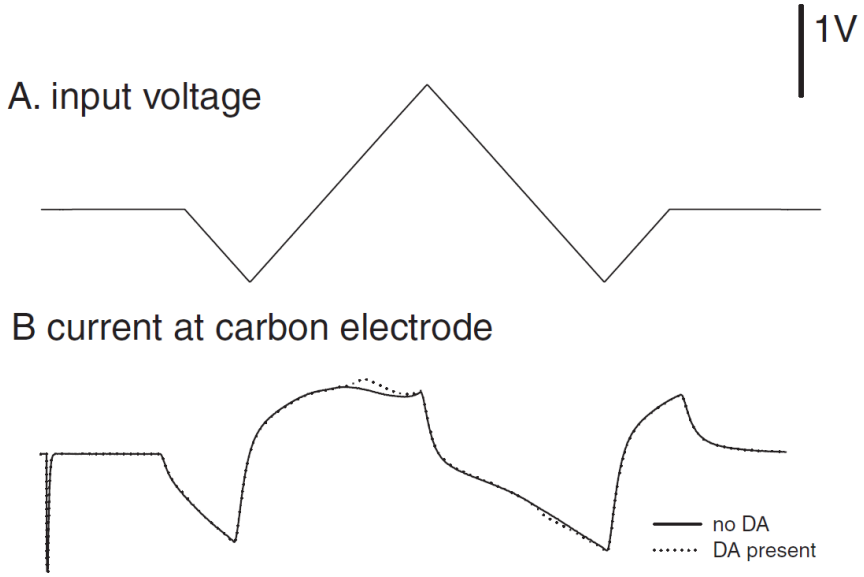

Figure 8. Voltammetric detection of OGD-evoked dopamine. (A) input voltage waveform to the carbon fibre electrode. The applied voltage consists of a triangular waveform, going from 0 to -1 then up to +1.4, back to -1 and then back to 0 V. (B) current evoked by the input voltage at the carbon fibre electrode. The solid line is the current prior to OGD-evoked dopamine efflux and the dotted line shows the current at peak dopamine efflux following OGD (From Davidson et al., 2011).

This technique offers some advantages, such as the possibility to measure endogenous dopamine (thus avoiding possible artefacts due to labelled-neurotransmitters overload that are commonly used in neurochemistry experiments) or the opportunity to evaluate "real-time" release with sub-second time resolution.

Effects of K_v7 modulators on anoxia-induced dopamine release

To investigate whether pharmacological modulation of K_v7 channels activity might interfere with the pathological consequences prompted by anoxia (possibly obtaining further information on the specific K_v7 subunit involved), we tested the effects of several drugs acting on K_v7 channels, provided with different subunit-specificity and pharmacological profile on OGD-induced dopamine release. Exposure of striatal slices to oxygen- and glucose- deprived artificial cerebrospinal fluid (OGD) causes a release of endogenous dopamine after about 8-10 minutes (time to onset, T-on), fastly reaching a peak (dopamine maximun concentration). Neural K_v7 activator retigabine, at the concentration of 1μM, delayed by about 30% such increase (130.62±7.35% with respect to control, thus determining an increase in time to onset), and also reduced dopamine peak (DA_{peak}) and rate of change of dopamine efflux (DA/T_{peak}), by about 40 and 60% respectively, when compared to vehicle-treated slices (DA_{peak} 56.54±12.01; DA/T_{peak} 39.83±8.93) (Fig.9).

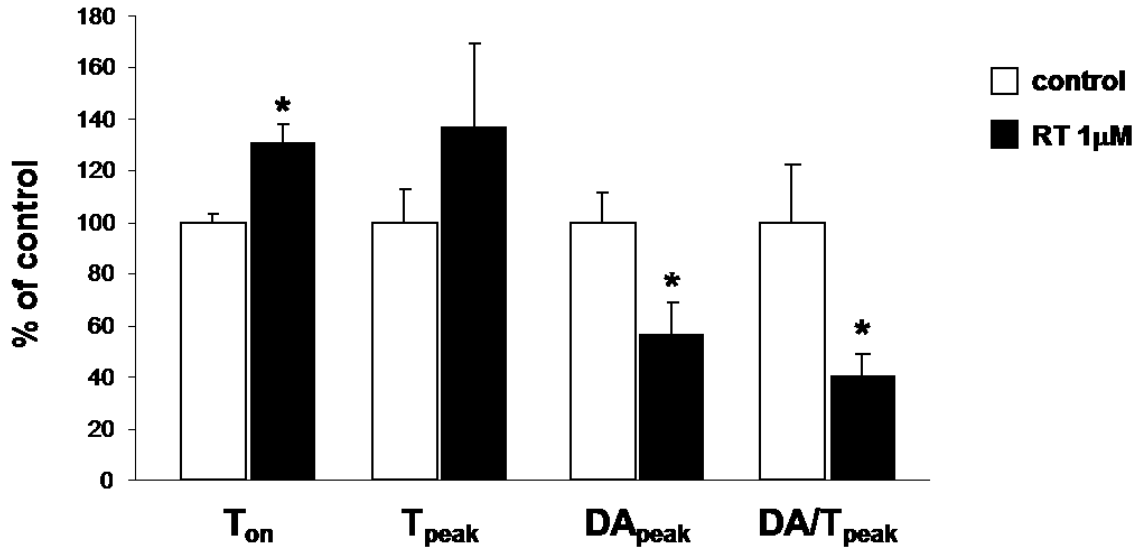

Figure 9. Effect of RT 1μM on voltammetric parameters. Data are expressed as % of DMSO-treated slices (control). Data are expressed as mean±S.E.M. (n=7 for both DMSO- and RT- treated slices). *=p<0.05

Another $K_v7.2/K_v7.3$-preferring activator, ICA27243, at the concentration of 1μM reduced dopamine peak by 60% (42.83±10.14% of control) while it did not significantly affect time to onset (101.60±18.90%). ICA27243 also reduced time to reaching dopamine peak by about 60%, although the speed to achieve

maximum dopamine concentration (rate of change of dopamine) was not significantly different when compared to control slices (T_{peak} 43.77±10.05%; DA/T_{peak} 120.72±34.74% with respect to controls) (Fig 10).

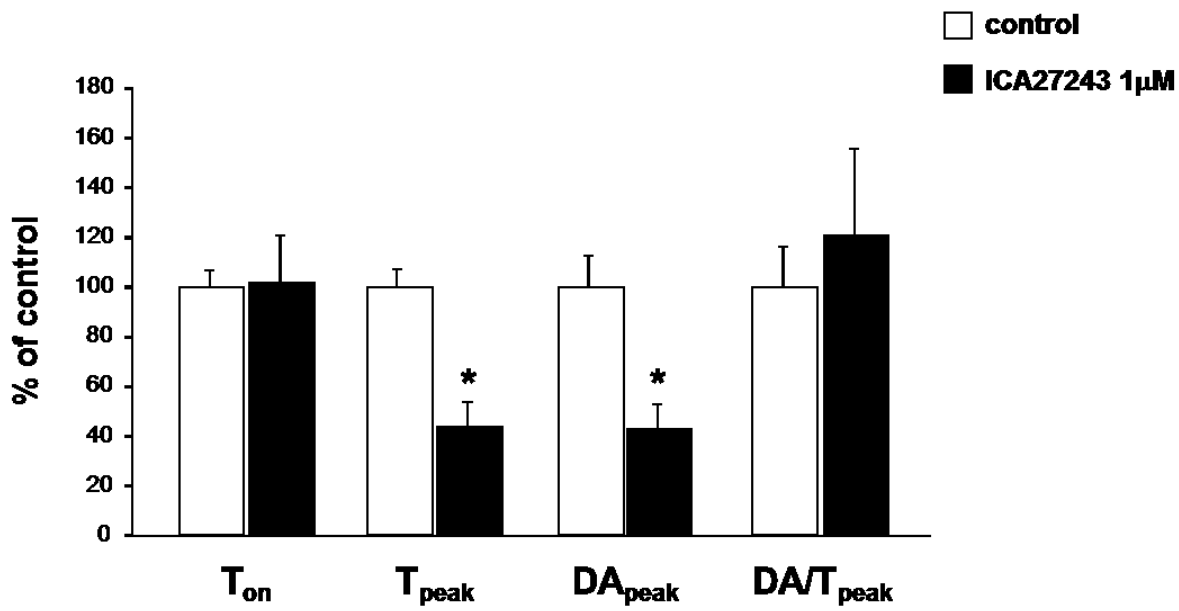

Figure 10. Effect of ICA27243 1µM on voltammetric parameters. Data are expressed as % of DMSO-treated slices (control). Data are expressed as mean±S.E.M. (n=6 for both DMSO- and ICA-treated slices). *=p<0.05

By contrast K_v7 activator NS15370 (a more potent K_v7 opener with respect to retigabine) at the concentration of 0.1µM almost doubled time to reach dopamine peak with respect to vehicle-treated slices (199.82±34.14%), but it showed no significant effects on other parameters (T-onset: 99.48±21.10; DA/T_{peak}: 91.21±35.92% vs controls) (Fig 11).

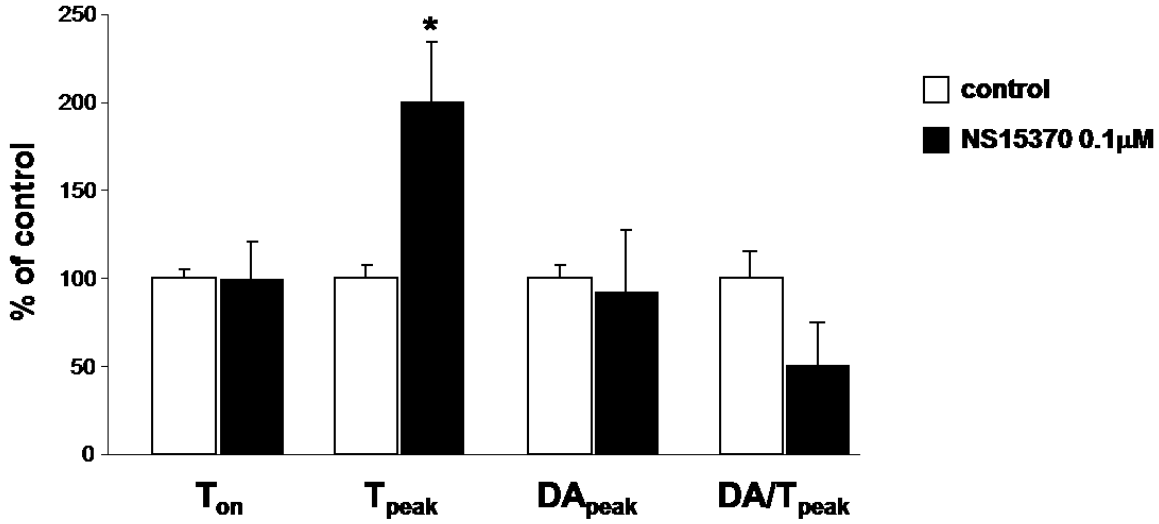

Figure 11. Effect of NS15370 0.1µM on voltammetric parameters. Data are expressed as % of DMSO-treated slices (control). Data are expressed as mean±S.E.M. (n=4 for both DMSO- and NS-treated slices). *=p<0.05

Then we tested two different pan-K_v7 blockers, in particular XE991, and linopiridine. While XE991, although causing a variable and not-significant increase the rate of change of dopamine (187.60±67.66%), did not interfere with dopamine release from caudate (103.65±8.92) (Fig 12), linopiridine 10 µM showed a 4-fold increase in dopamine peak and rate of dopamine, thus suggesting a possible neurotoxic effect of K_v7 channels blockade (DA_{peak} 417.19±84.89%; DA/T_{peak} 435.60±75.13% with respect to controls) (Fig 13).

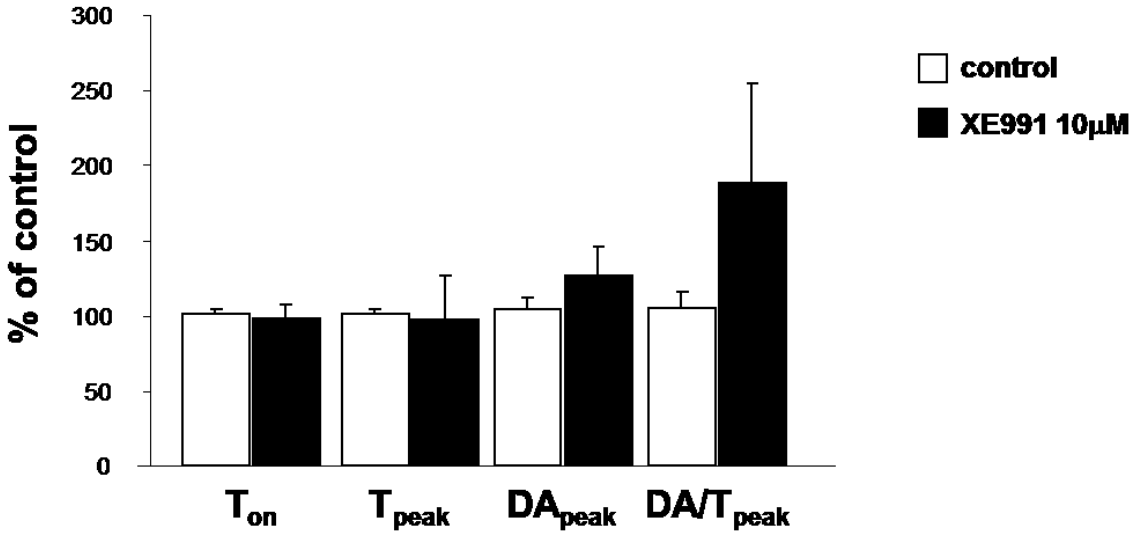

Figure 12. Effect of XE991 10µM on voltammetric parameters. Data are expressed as % of DMSO-treated slices (control). Data are expressed as mean±S.E.M. (n=7 for both DMSO- and XE991- treated slices). *=p<0.05

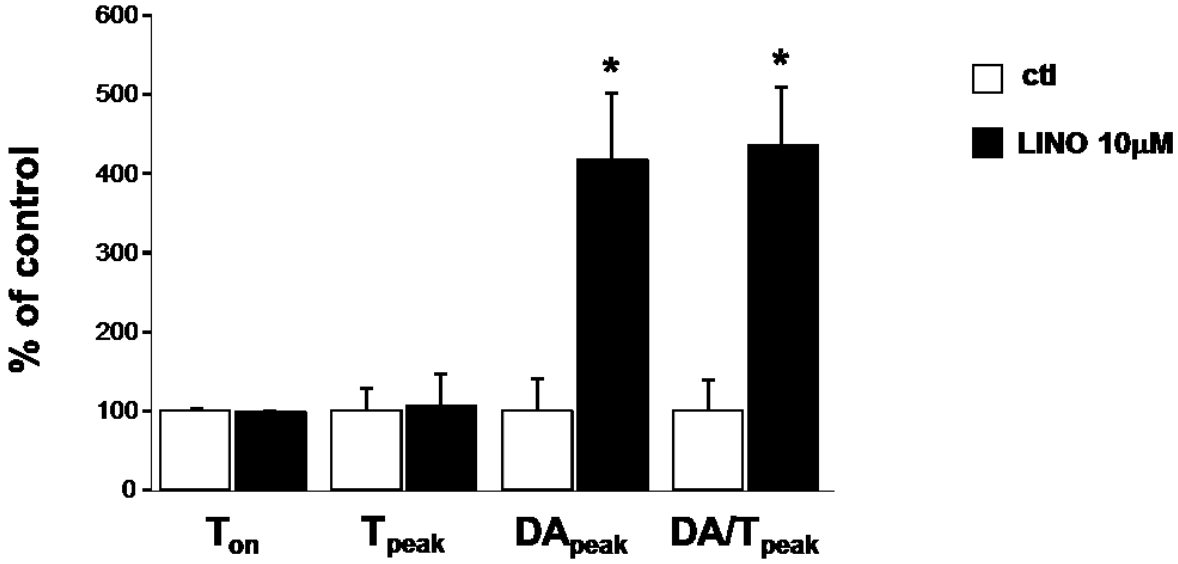

Figure 13. Effect of linopiridine 10µM on voltammetric parameters. Data are expressed as % of DMSO-treated slices (control). Data are expressed as mean±S.E.M. (n=7 for both DMSO- and LINO- treated slices). *=p<0.05

In addition, when incubated together with retigabine, Linopiridine 10µM was able to prevent the changes in time to onset, dopamine maximum concentration and rate of change of dopamine release induced by retigabine after OGD superfusion (Fig14).

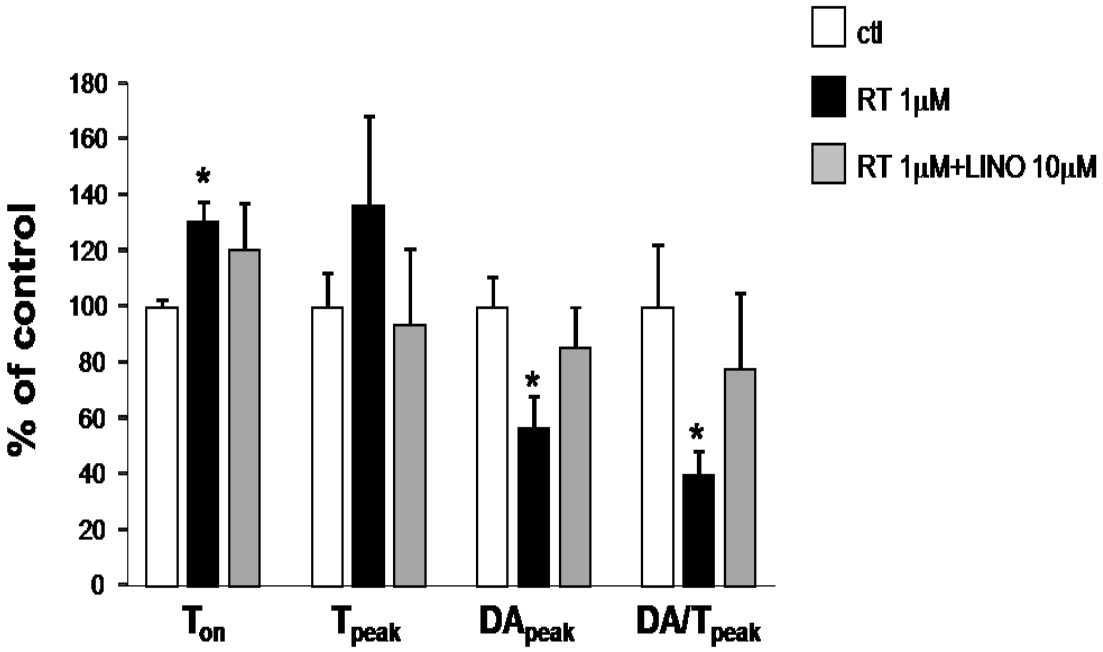

Figure 14. Effect of linopiridine 10μM co-incubated with retigabine1μM on voltammetric parameters. Data are expressed as % of DMSO-treated slices (control). Data are expressed as mean±S.E.M. (n=5 for both DMSO- and LINO- treated slices). *=p<0.05

Effects of K_v7 modulators on anoxia-induced damage

To further investigate whether the reduced dopamine release caused by K_v7 activators could determine also a decrease in on brain slices damage induced by OGD, we performed TTC staining experiments, a widely-used and fast method to measure cell viability in histological sections. In these experiments, brain slices were incubated in normal aCSF for 30 minutes after the OGD insult, to allow brain damage to be evaluated. Exposure of brain slices to OGD medium caused a loss in TTC staining compared to control slices by about 40% (61.80±4.68% with respect to control). Retigabine (at concentrations ranging from 0.3 to 10μM) was able to reduce the loss of TTC staining induced by OGD, in a dose-dependent manner, with the higher effect shown at concentrations of 10μM (84.27±9.17% versus control) (Fig15).

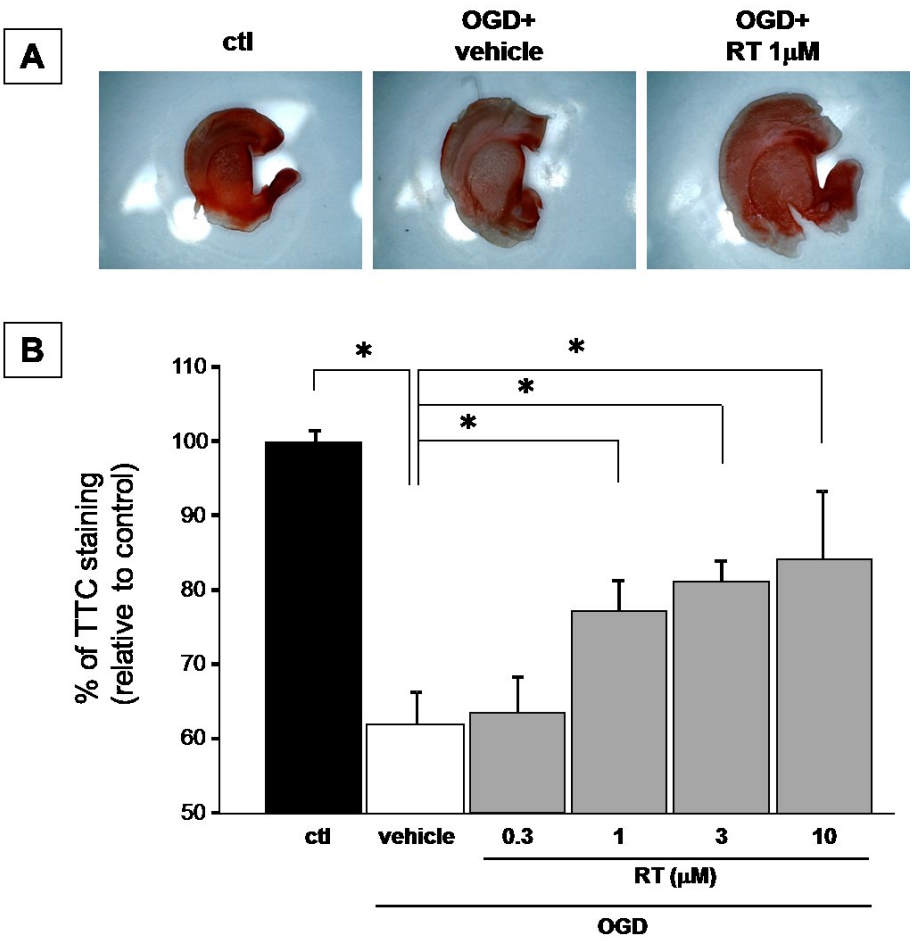

Figure 15. (A) Representative images showing TTC staining on brain slices incubated in normal aCSF (ctl), OGD+vehicle or OGD+RT 1μM. (B) Quantification of the effects on TTC staining exerted by increasing concentrations of retigabine in OGD-exposed slices. Data are expressed as % of normal aCSF-incubated slices (control). Data are expressed as mean±S.E.M. (n= at least 5 for each experimental point). *=$p<0.05$

Moreover, ICA27243 (at concentration ranging from 0.1 to 10μM) dose-dependently prevented the loss of TTC staining in brain slices exposed to OGD (vehicle-treated slice: 69.64±2.06%; ICA27243 10μM-treated: 89.06±8.64% with respect to control) (Fig 16).

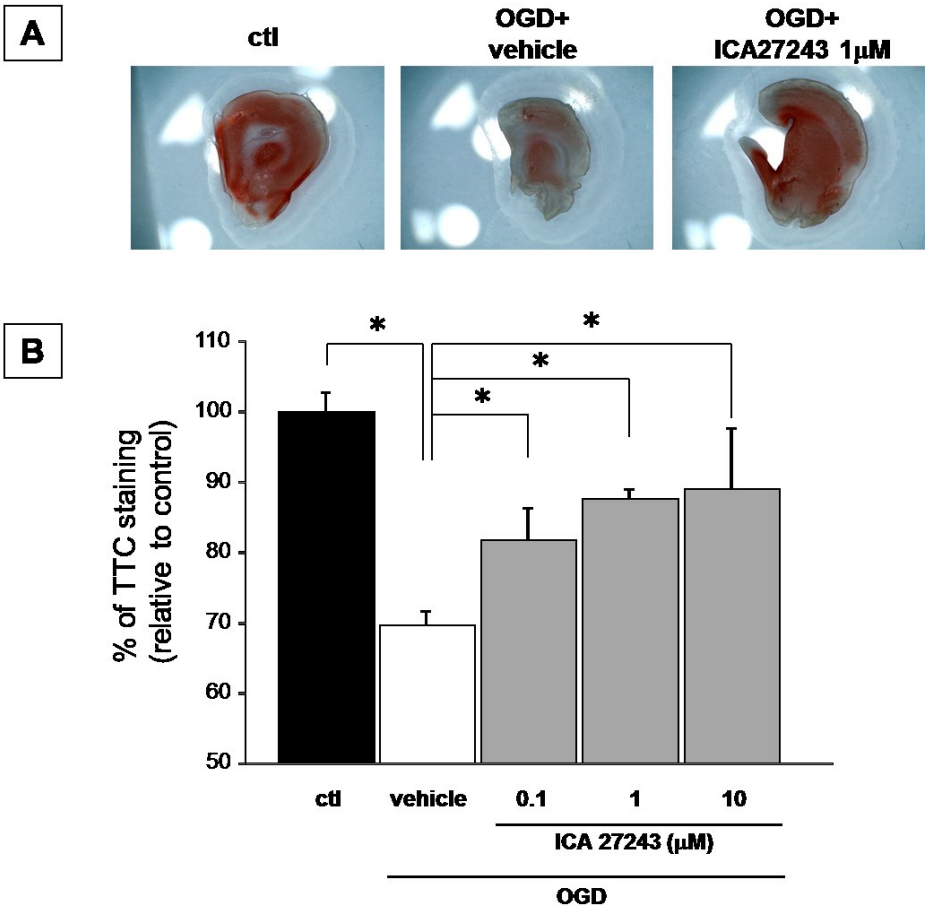

Figure 16. (A) Representative images showing TTC staining on brain slices incubated in normal aCSF (ctl), OGD+vehicle or OGD+ICA27243 1µM. (B) Quantification of the effects on TTC staining exerted by increasing concentrations of ICA27243 in OGD-exposed slices. Data are expressed as % of normal aCSF-incubated slices (control). Data are expressed as mean±S.E.M. (n= at least 5 for each experimental point). *=p<0.05

By contrast, exposure of brain slices to different concentrations of linopiridine did not have any effect at lower doses, but it enhanced OGD-induced loss of TTC staining only at the higher concentration tested (30µM; 60.26±6.16% compared to 80.23±3.65% of vehicle-treated slice) (Fig17).

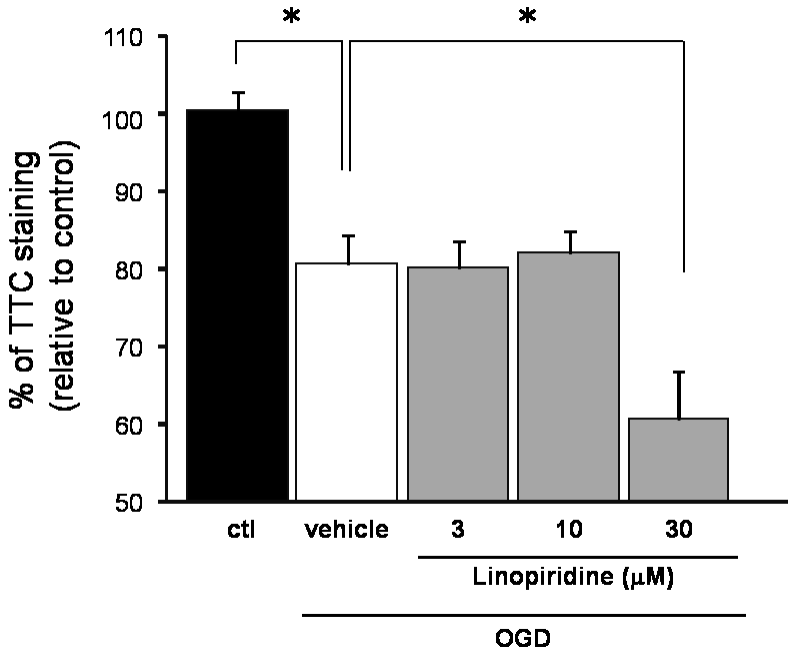

Figure 17. Quantification of the effects on TTC staining exerted by increasing concentrations of Linopiridine in OGD-exposed slices. Data are expressed as % of normal aCSF-incubated slices (control). Data are expressed as mean±S.E.M. (n= at least 5 for each experimental point). *=p<0.05

Moreover, co-incubation of Linopiridine 10μM reversed the reduction in loss of TTC-staining exerted by retigabine at the concentration of 1μM (Fig18).

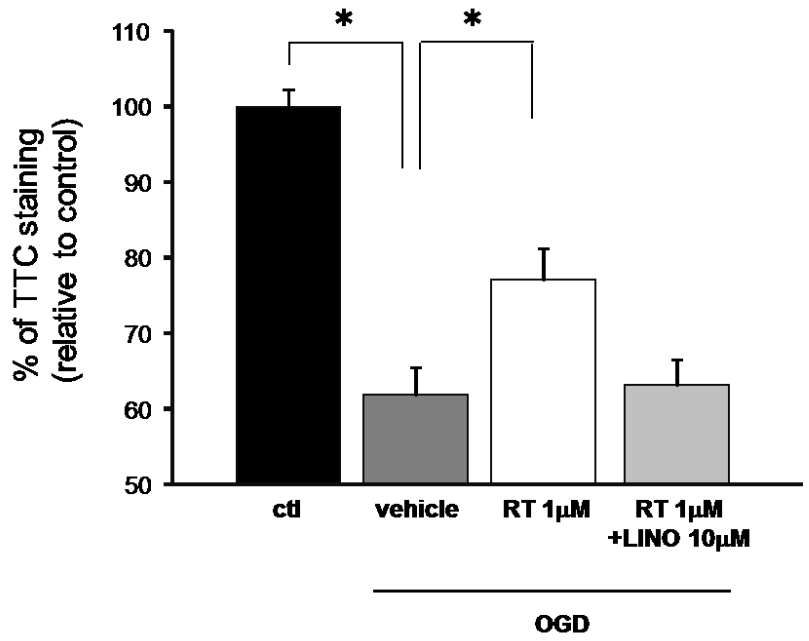

Figure 18. Quantification of the effects on TTC staining exerted by RT 1μM and RT 1μM+Linopiridine 10μM in OGD-exposed slices. Data are expressed as % of normal aCSF-incubated slices (control). Data are expressed as mean±S.E.M. (n= at least 5 for each experimental point). *=p<0.05

Effects of anoxia-reoxygenation on K_v7 channels expression

Since activation of M-current seems to reduce damage induced by anoxia and glucose deprivation, possibly with slight differences depending on the compound used and its subunit-selectivity, we next evaluated the possible changes in K_v7 subunits expression levels after OGD insults. Exposure of striatal brain slices to (OGD) for 15 minutes and subsequet incubation in normal artificial cerebrospinal (aCSF) fluid for 30 minutes caused a ~6-fold decrease in the trascript of $K_v7.2$ gene measured by real-time PCR; levels of mRNAs encoding for other K_v7 subunits seemed to be unaffected by anoxia-reperfusion insult (Fig 19A). Western blot experiments showed a parallel, although less evident, reduction in $K_v7.2$ protein levels in brain slices exposed to OGD (by about 50%) (Fig 19B).

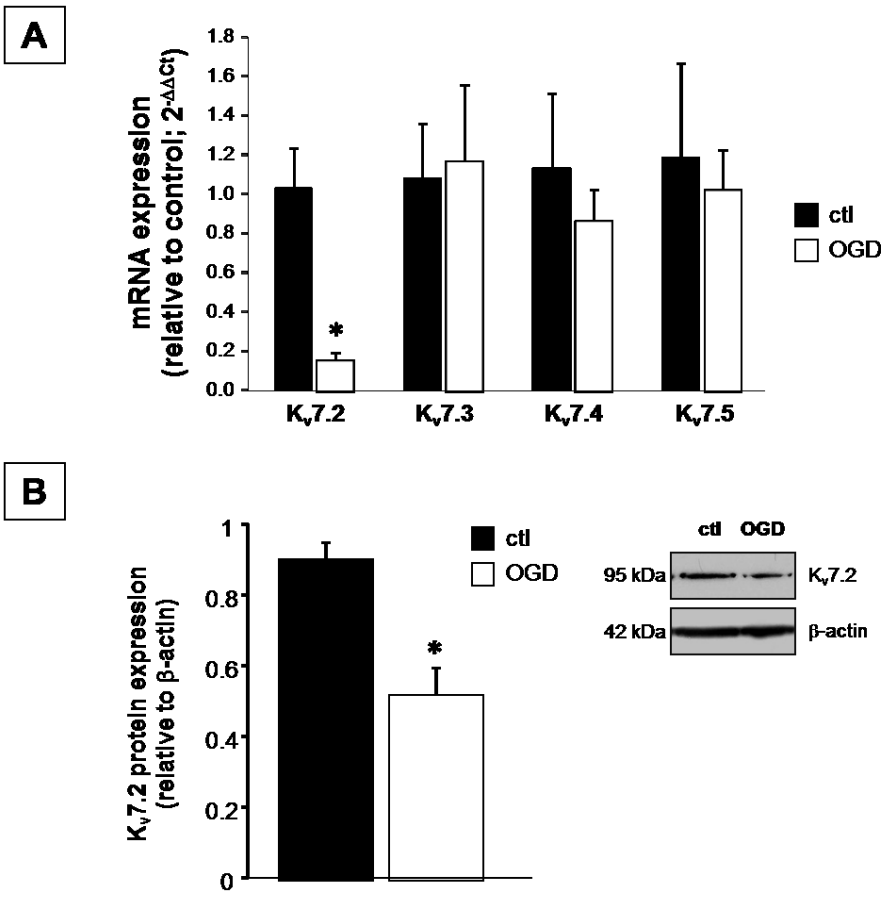

Figure 19. (A) Quantification of mRNA levels encoding for Kv7 subunits in striatal slices exposed to normal aCSF (control) or OGD. Data are normalized to housekeeping gene (gapdh) and expressed as relative to the average of controls, using the $2^{-\Delta\Delta Ct}$ formula. Data are expressed as mean±S.E.M. (n= 5 for both control abd OGD slices). *=p<0.05. (B) Western blot analysis for Kv7.2 protein expression on total lysates from control- or OGD-treated slices. The inset shows a representative blot for Kv7.2 and β-actin. The approximate molecular mass for each of these proteins (expressed in kDa) is shown on the left. Bar graph shows the quantification of the averaged OD values for the Kv7.2 bands, normalized to the OD value for β-actin, in both control- (solid columns) and OGD-exposed (open columns) slices. *p ≤ 0.05 vs. respective control; n=5 for both control- and OGD-exposed slices.

K_V7.2 and encephalopathy

The results shown before suggest that changes in the activity of K_v7 channels might represent a relevant event in the pathological cascade leading to brain dysfunction and damage. This potential role of K_v7 channels, in particular K_v7.2, is underlined by the finding that mutations in K_v7.2 gene can lead not only to BFNS, but also to severe form of neuronal diseases, such as pharmacoresistant epilepsy or encephalopathy. Such heterogeneous phenotypes might be due to

distinct mutations, differently affecting channel function. To better understand this phenomenon, we investigated the functional changes prompted by two mutations in the fifth arginine residue of the S4 transmembrane domain belonging to the voltage sensing domain of K_v7.2 channel (R213 or R6). This residue, together with other positively-charged aminoacid in the S4 segment, is highly conserved among different potassium channels and play a fundamental role in sensing changes of membrane potential, thus causing the channel gating (Fig20).

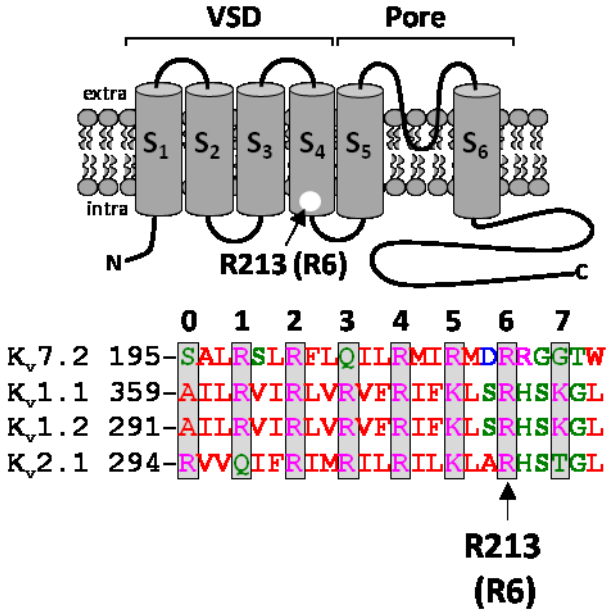

Figure 20. Topological representation of a Kv7.2 subunit (top) and equence alignment of the S4 segments of the indicated Kv subunits (bottom), with the R213 (R6) residue highlighted. Residues are colored according to the following scheme: magenta, basic; blue, acid; red, nonpolar; and green, polar.

Patch clamp recordings in CHO cells transfected with wild type or mutant K_v7.2 channels showed that the substitution of arginine residue with a tryptophan (R6W) or a glutamine (R6Q) did not cause a significant change in maximal density of currents when compared to wild type (wt) K_v7.2 channel, thus suggesting that plasma-membrane expression of the mutant proteins were not affected. Indeed, current densities were 25.9±3.8 pA/pF for wild type subunit, 24.8±4.5 pA/pF and 33.9±8.1 pA/pF for K_v7.2-R6W and K_v7.2-R6Q, respectively. By contrast, both mutations caused a significant decrease in the voltage

sensitivity of the channel, with R6Q substitution showing a higher reduction compared to R6W. The half activation potential ($V_{1/2}$) was −23 mV in KV7.2 channels; this value was right-shifted by 58 mV and 68 mV in R6W and R6Q mutant channels, respectively (Fig21).

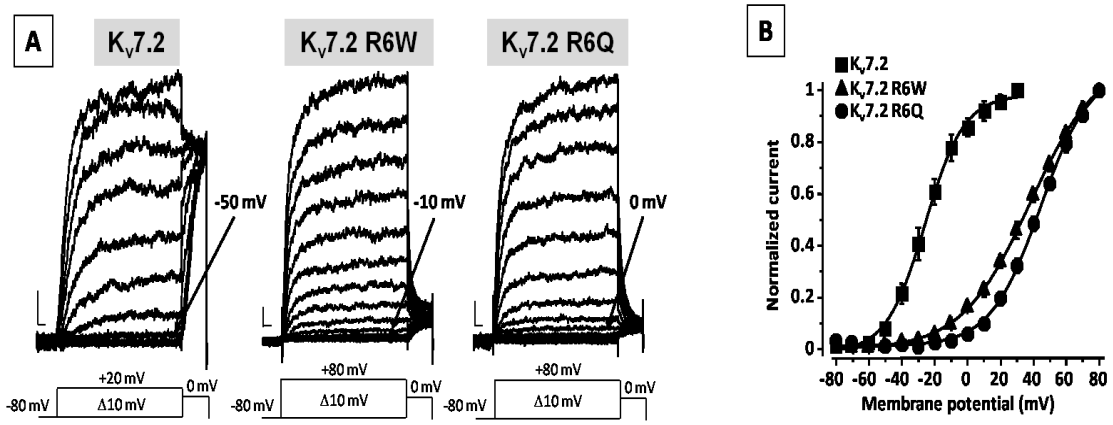

Figure 21. (A) Macroscopic currents from K_V7.2, K_V7.2 R6W, and K_V7.2 R6Q channels, in response to the indicated voltage protocols. Current scale, 100 pA; time scale, 0.1 s. The arrows indicate the threshold voltage for current activation. (B) Conductance/ voltage curves. Continuous lines are Boltzmann fits to the experimental data.

Since in neuronal cells M current is underlied by homo- or hetero- meric assembly of K_v7.2 and K_v7.3 subunits, we investigated the functional consequence of the incorporation of mutated proteins in the tetrameric channel. Moreover, to reproduce the genetic balance of the patients affected (who are heterozygous for the mutant allele) and normal individuals, we transfected CHO cells with K_v7.2 and K_v7.3 plasmids in different ratios; in particular, we used wt K_v7.2 and K_v7.3 in a 1:1 ratio to reproduce the phenotype of normal individuals, and wt K_v7.2+K_v7.2R6W+K_v7.3 or wt K_v7.2+K_v7.2 R6Q+K_v7.3 (0.5:0.5:1 ratio) to mimic the genetic balance of affected patients (Fig22).

Heteromeric channels composed by K_v7.2 and K_v7.3 subunits show larger current compared to homomeric tetramers. As for mutated channels in homomeric conformation, heteromeric channels formed by K_v7.2R6W or K_v7.2R6Q did not display a decrease in macroscopic currents with respect to wt K_v7.2, suggesting that they did not interfere with heteromeric assembly and/or

trafficking to the plasma membrane (current densities were 110.8±20.7 pA/pF for $K_v7.2$+$K_v7.3$; 98.8±12.5 pA/pF for $K_v7.2$+$K_v7.2$R6W+$K_v7.3$; and 85.0±17.9 pA/pF for $K_v7.2$+$K_v7.2$R6Q+$K_v7.3$) (Fig22A). Moreover, a right-shift in the voltage dependence of channels incorporating mutated subunit was observed, with R6Q showing a more dramatic effect when compared to R6W ($V_{1/2}$ were −30.7±1.4 for $K_v7.2$+$K_v7.3$; −22.2±2.0 for $K_v7.2$+$K_v7.2$R6W+$K_v7.3$; −14.7±2.6 for $K_v7.2$+$K_v7.2$R6Q+$K_v7.3$). Such a decreased voltage sensitivity determined by the arginine substitutions was also evident in $K_v7.2$ channels in homomeric conformation, a channel composition that has been demonstrated to occur at specific neuronal sites and during early stages of development. Indeed, transfection of CHO cells with wt and mutated $K_v7.2$ subunit in 1:1 ratio caused a right shift in voltage-sensitivity of R6W and R6Q $K_v7.2$ channels when compared to channels composed by wt $K_v7.2$ ($V_{1/2}$ were −22.9±1.8 for wild-type channels; −6.8±3.1 for $K_v7.2$wt+$K_v7.2$R6W; 17.7±3.3 for $K_v7.2$wt+$K_v7.2$R6Q) (Fig 22B and C).

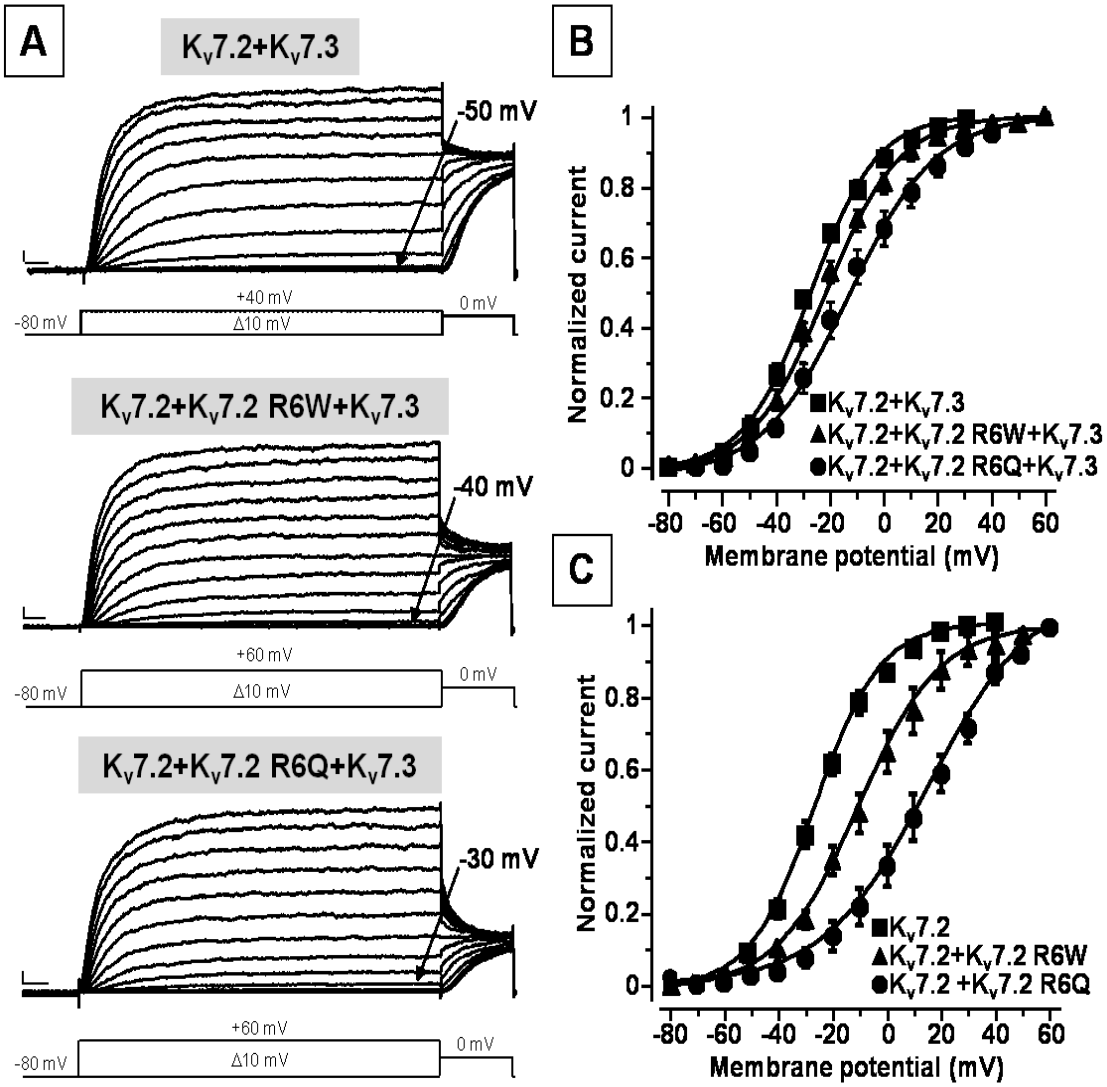

Figure 22. (A) Macroscopic current traces from the indicated heteromeric channels in response to the indicated voltage protocols. Current scale, 200 pA; time scale, 0.1 s Arrows indicate the threshold voltage for current activation. (B and C) Conductance/voltage curves for the heteromeric channels formed by mutant subunits with wild type $K_V7.2$ and $K_V7.3$ (B) or with wild type $K_V7.2$ (C). Continuous lines are Boltzmann fits to the experimental data.

To assess the possible effects of the changes in the properties of heteromeric $K_V7.2$ channels induced by R6 aminoacid changes, we introduced the biophysical parameters derived from patch-clamp experiments in a model CA1 hippocampal neuron. In this model we evaluated the changes in neuron excitability prompted by mutations by measuring the voltage responses and the number of action potentials generated in response to a wide range of injected current (between 0.3 and 0.7 nA). While CA1 neuron incorporating R6W showed only a slightly increase in the number of spikes after current with respect to wt,

mutant R6Q CA1 neuron responded with a higher number of spikes when compared to wt (Fig23A). Moreover, a higher number of action potential was observed for R6Q mutation also at relatively low current injection values, while, channels incorporating K_V7.2-R6W subunit caused similar effects only for larger input currents (Fig23B).

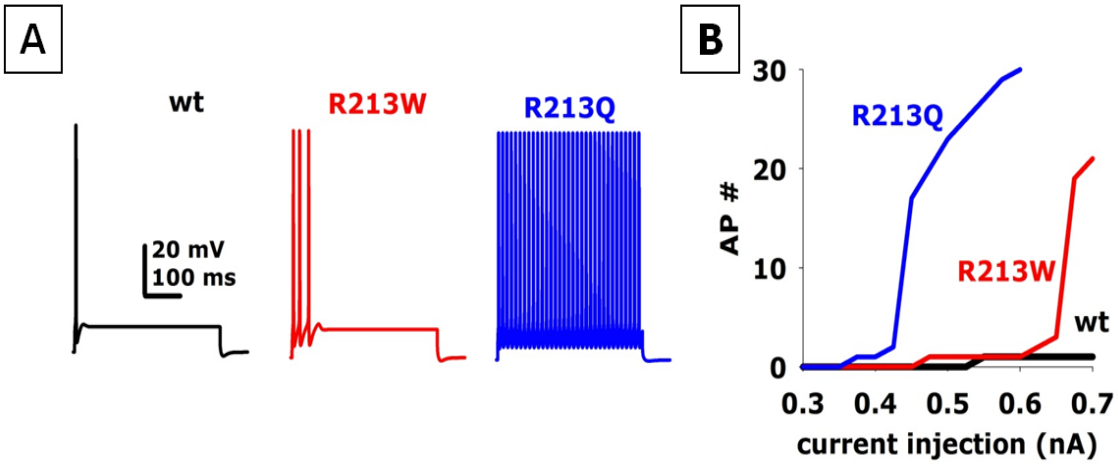

Figure 23. Modeling of the effects of the K_V7.2 R213W (R6W) and R213Q (R6Q) mutations on neuronal excitability. (A) Time courses of the somatic membrane potential from CA1 neurons expressing K_V7.2+K_V7.3 (black lines), K_V7.2+K_V7.2 R6W+K_V7.3 (red lines), or K_V7.2+K_V7.2 R6Q+K_V7.3 (blue lines) heteromeric channels, during a 500-ms somatic current injection of 0.65 nA. (B) Input/output (I/O) curves from cells expressing K_V7.2+K_V7.3 (black line), K_V7.2+K_V7.2 R6W+K_V7.3 (red line), or K_V7.2+K_V7.2 R6Q+K_V7.3 (blue line) heteromeric channels. Number of APs (AP#) is expressed as a function of the somatic current injected, using a 120 mS/μm2 peak IKM conductance.

We then investigated if the functional changes determined by mutation in R6 residue could be rescued by retigabine, a K_V7 activator able to increase M current (among other mechanisms) also by causing a left-shift in channel voltage sensitivity. Retigabine used at the concentration of 1μM was able to fully reverse the effects on channel gating induced by mutations, thus bringing the voltage sensitivity of mutated channels to that of wild type (Fig24).

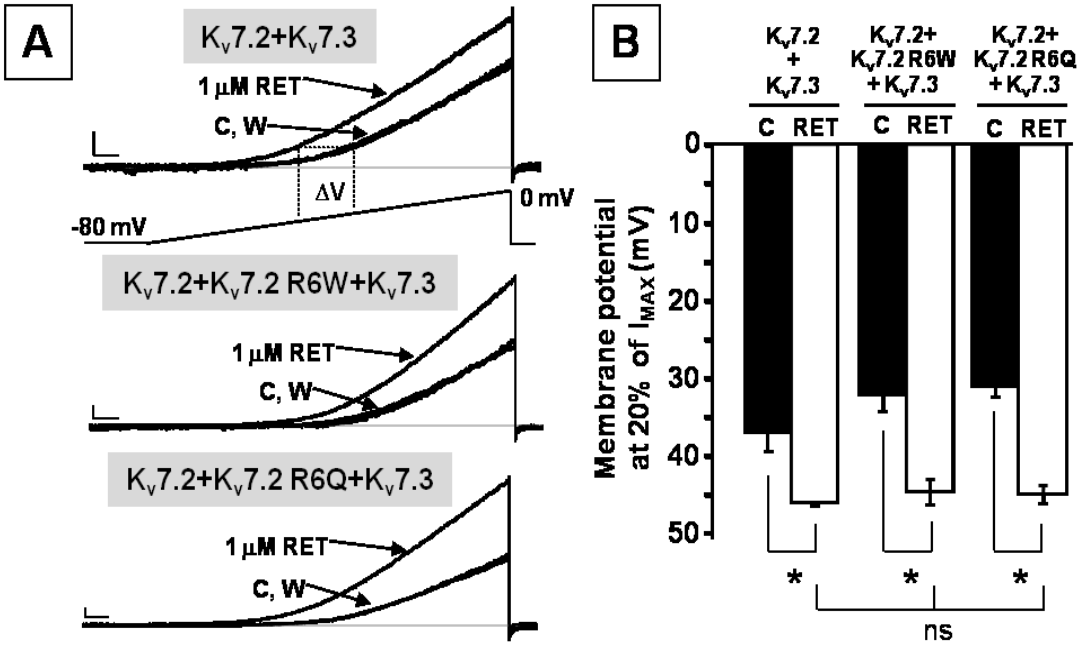

Figure 24. Effect of retigabine on heteromeric $K_V7.2+K_V7.3$, $K_V7.2+K_V7.2$ R6W+$K_V7.3$, or $K_V7.2+K_V7.2$ R6Q+$K_V7.3$ channels. (A) Current responses from the indicated heteromeric channels to voltage ramps from −80 to 0 mV. C, control currents; RET, retigabine; W, washout. Current scale, 200 pA; time scale, 0.2 s. (B) Quantification of the effects of RET on the indicated heteromeric channels. Data are expressed as membrane potentials at which currents reached 20% of their peak value for controls (black bars) and after RET exposure (white bars). *P < 0.05 vs. corresponding controls; ns, not significantly different). Current scale, 200 pA; time scale, 200 ms.

DISCUSSION

Ionic homeostasis is a primary goal for excitable cells as neurons, as alterations of the concentrations of different ionic species is both a cause and a consequence of different pathological processes (apoptosis, cell shrinkage, proteases activation) and diseases. In particular, K^+ ions imbalance seems to be strictly linked to neuronal dysfunction, also for the pivotal role exerted in determining resting potential and cell excitability. Indeed, hyper-excitability is a common feature of many diseases such as epilepsy and ischemia; as a consequence, K^+ channels are important regulators of neuronal activity and their modulation might have important consequences on neurons death/survival. Among them, voltage-gated K^+ channels belonging to K_v7 family have gained increasing interest since mutations in genes encoding for $K_v7.2$ and $K_v7.3$ subunits were discovered to cause an inherited form of epilepsy called BFNS (Singh et al, 1998; Charlier et al, 1998; Bievert et al, 1998). Subsequently, the physiological relevance of K_v7 channels and M-current has been better defined, with several studies demonstrating its role in neuronal excitability regulation at somato-dendritic, nodal and pre-synaptic levels, thus modulating different processes such as neurotransmitters release. Massive neurotransmitters release occurs during brain ischemia, possibly due to damage-induced depolarisation and/or rising of intracellular Ca^{2+} concentrations (Doyle et al., 2008). In particular, dopamine release has been demonstrated to reach very high levels soon after an ischemic insult and also to contribute to neuronal damage. Given the known effect of K_v7 activator retigabine in reducing dopamine release in isolated nerve terminals (Martire et al., 2007), in this study we investigated the possibility that pharmacological activation of K_v7-mediated currents could exert neuroprotective effects in a in vitro model of ischemia. In particular, we focused on striatum, a region receiving dopaminergic projections from mesencephalic substantia nigra, and frequently damaged in ischemic stroke in humans (for the occlusion of the middle cerebral artery).

In our experiments retigabine was able to reduce dopamine release induced by exposure of striatal brain slices to aCSF deprived of glucose and oxygen;

moreover, retigabine also delayed dopamine time to onset and slowed down the release. This is particularly relevant, since previous studies have shown that putative neuroprotective agents increased time to onset in rat brain slices, thus suggesting that delay in this parameter is a good indicator of neuroprotection (Toner et al., 2001). Moreover, retigabine exerted its action at the concentration (1μM) that is very close to the EC_{50} for the activation of $K_v7.2/K_v7.3$ heteromers, which are thought to be the most frequent channels composition underlying M-current in brain (Cooper et al., 2000). Neuroprotective actions of retigabine were also confirmed by TTC staining experiments, in which neuronal damage has been measured by evaluating the mitochondrial dysfunction induced by OGD insult. Retigabine dose-dependently reduced brain damage induced by OGD, showing a considerable effect also at the concentration of 1μM. The potential neuroprotective effects of K_v7 channels activation was also confirmed by the results obtained using ICA27243, a compound provided with higher subunit selectivity, showing a higher potency on $K_v7.2/K_v7.3$ heterotetramers. Although time to onset was not delayed, ICA27243 1μM did significantly reduce dopamine levels reached after OGD insult, thus possibly preventing the detrimental consequences of such a huge release. Indeed, exposure of brain slices to different concentrations of ICA27243 reduced brain damage measured by TTC staining, with an effect quantitatively similar to that determined by retigabine. By contrast, NS15370 1μM was not able to reproduce the same effects on dopamine release obtained with retigabine and ICA27243, which is apparently contradicting. However, it should be mentioned that NS15370, although more potent than retigabine, has a very complex effect, showing also K_v7 channel blockade at depolarized potential (Dalby-Brown et al., 2013), a characteristic that might in part explain the lack of effects in dopamine release modulation. Consistent with the previous observations, pharmacological blockade of K_v7 channel by linopiridine 10μM increased and hastened dopamine release; this result was paralleled, at least in part, by the worsening of OGD-induced brain damage caused by exposure to linopirine, although at higher concentration (30μM) than those able to increase dopamine release. Moreover, linopiridine 10μM was able to reverse the changes in dopamine release induced

by retigabine, as well as the reduction in TTC staining loss induced by the K_v7 activator. Linopiridine-induced increase of dopamine release was not completely reproduced by its analogue XE-991 (10μM), since the latter caused only a slight increase in dopamine peak and in rate of change, without being significantly different. Interestingly, XE-991 has been demonstrated to increase depolarization-induced dopamine release from isolated striatal nerve endings (Martire et al., 2007), but showed no or low efficacy in increasing cortical aspartate (Luisi et al., 2009) or hippocampal noradrenaline (Martire et al., 2004) release from synaptosomes. Differences in the experimental models (isolated terminals vs brain slices), as well as in drug pharmacological properties and doses might explain this discrepancy.

Moreover, both qPCR and western blot data showed a decrease in $K_v7.2$ subunit expression after OGD insult, both at transcripts and protein levels. This reduction seems to affect only $K_v7.2$, since transcript levels for other K_v7 subunits are not significantly different from control condition. Although we do not know whether this reduction is a possible pathogenetic mechanism or merely a consequence of ischemic damage, pharmacological data suggest that M-current mediated by $K_v7.2$ subunit might counteract abnormal changes prompted by ischemia and, at least in part, protect from brain damage. Moreover, it has been demonstrated that in striatal synaptosomes selective $K_v7.2$ blockade with a subunit-specific antibody was able to completely abolish the decrease of dopamine release induced by retigabine (Martire et al., 2007), suggesting a primary role of $K_v7.2$ subunits as molecular determinants of M-current in this brain area .

Taken together, these results might suggest a main role for $K_v7.2$ also in the modulation of dopamine release induced by an ischemic insult. Pharmacological activation of M-current, possibly by counteracting the depolarization-induced release of neurotransmitters following ischemia, as well as by restoring I_{KM}, might represent a useful a new strategy for the treatment of brain ischemia.

Kv7.2 and encephalophathy

As stated before, the pathological role of K_v7.2 is highlighted by genetic disease associated to mutations affecting its function. Although in most cases alterations of K_v7.2 are responsible for BFNS, a dominantly-inherited neonatal epilepsy with generally a favorable outcome, novel mutations have been recently identified in children with severe forms of epileptic encephalopathies and variable psychomotor impairment (Weckhuysen et al., 2012; Saitsu et al., 2012). Molecular basis for this phenotypic variability is yet unknown, but it has been hypothesized that specific aminoacid substitutions might prompt different functional consequences, thus possibly explaining such variability. To further investigate this hypotesis, in the present study we have evaluated the molecular pathogenesis of channel dysfunction caused by two mutations affecting the fifth arginine of K_V7.2-VSD, and responsible for epileptic encephalopathy (R6Q)(Weckhuysen et al., 2012), or for BFNS (R6W) (Sadewa et al., 2012). Macroscopic current analysis in transfected cells revealed that both mutations, in homomeric or heteromeric configuration with K_V7.2 and/or K_V7.3, did not modify the maximal current density, suggesting that they did not interfere with channel expression to plasma membrane. By contrast, both mutated channels showed a remarkable decrease in their voltage sensitivity, with a more dramatic effect for R6Q when compared with the R6W mutation. The shift in voltage sensitivity was maximal in mutant homomeric configuration (four mutant subunits), intermediate in homomeric configuration with wild type K_V7.2 subunits or in heteromeric configuration with K_V7.3 subunits (two mutant subunits), and smaller in heteromeric channels reproducing the genetic balance of affected individuals (one mutant subunits), thus suggesting that the degree of reduction in voltage-sensitivity strongly depended on the number of mutant subunit incorporated. The shift in voltage-sensitivity caused by R6W mutation was qualitatively and quantitatively similar to that of previously described BFNS mutations (Castaldo et al., 2002: Miceli et al., 2009). By contrast, changes determined by R6Q subunit, was the most dramatic among the functional changes described in K_V7.2 channelopathies (Bellini et al., 2010). Such dramatic effects were observed both in homomeric conformation with K_v7.2 (a channel

composition that has been suggested to occur in key-sites such as Ranvier nodes and possibly at pre-synaptic sites), as well as in the heteromeric configuration mimicking the genetic balance of the affected individual. Computational results from a CA1 model of hippocampal neuron confirmed the higher severity of R6Q mutation; indeed, although both mutations increased neuronal excitability, incorporation of a single R6Q in heteromeric configuration with $K_V7.2$ and $K_V7.3$ subunits, dramatically increased neuronal firing, with an effect significantly higher than that produced by R6W mutation. Interestingly, retigabine, at clinically relevant concentrations (Gunthorpe et al., 2012; Hermann et al., 2003), was able to restore normal function in both R6Q and R6W channels, by shifting voltage-dependence of these channels to values similar to wild-type subunits. Collectively, these results suggest that the more severe phenotype associated to R6Q mutation might be due to a greater functional impairment on channel activity and in particular on gating properties caused by the mutation, thus giving a genotype–phenotype correlation in $K_V7.2$-linked channelopathies. Moreover, efficacy of retigabine in counteracting the abnormal changes prompted by the mutation might also have relevant impact on treatment of this disease; this is particularly important in children, in consideration of the fact that most first-line drugs given to neonates to treat seizures (usually phenobarbital and phenytoin) are effective in less than 50% of cases, and concerns about their administration to children has emerged since they have been demonstrated to cause widespread neuronal apoptosis when given to young rodents (Painter et al., 1999).

Taken together, these data suggest that K_v7 channels might play a key pathogenetic role in regulation of neuronal dysfunction characterized by hyper-excitability, and in the sequence of events that lead to severe brain damage and neurodegeneration, possibly by counteracting neuronal hyper-excitability and consequent massive dopamine (and other neurotransmitter) release occurring in this pathological condition. Moreover, pharmacological enhancement of M-current exerts neuroprotective effects in in vitro model of brain ischemia, and fully revert the alterations in biophysics propertiers of channels caused by

mutations. Thus, pharmacological modulation of K_v7 channels might represent a unique tool to counteract hyperexcitability dysfunction.

REFERENCES

Aguilar-Bryan L, Nichols CG, Wechsler SW, Clement JP 4th, Boyd AE 3rd, González G, Herrera-Sosa H, Nguy K, Bryan J, Nelson DA. (1995). Cloning of the beta cell high-affinity sulfonylurea receptor: a regulator of insulin secretion. Science. 268(5209):423-6

Armstrong CM, Bezanilla F (1974). Charge movement associated with the opening and closing of the activation gates of the Na channels. J Gen Physiol 63: 533-552

Arumugam, TV, Okun E, Mattson MP (2009). Basis of Ionic Dysregulation in Cerebral Ischemia. In: New Strategies in Stroke Intervention, editor L Annunziato Springer, Berlin; Humana Press.

Bellini G, Miceli F, Soldovieri MV, et al. KCNQ2-Related Disorders. 2010 Apr 27 [Updated 2013 Apr 11]. In: Pagon RA, Adam MP, Bird TD, et al., editors. GeneReviews® [Internet]. Seattle (WA): University of Washington, Seattle; 1993-2014. Available from: http://www.ncbi.nlm.nih.gov/books/NBK32534/

Bendahhou S, Fournier E, Sternberg D, Bassez G, Furby A, Sereni C, Donaldson MR, Larroque MM, Fontaine B, Barhanin J. (2005). In vivo and in vitro functional characterization of Andersen's syndrome mutations. J Physiol 565: 731–741.

Bennett K, James C, Hussain K (2010). Pancreatic β-cell KATP channels: Hypoglycaemia and hyperglycaemia. Rev Endocr Metab Disord. 11:157-63

Bentzen BH, Schmitt N, Calloe K, Dalby Brown W, Grunnet M, Olesen SP (2006). The acrylamide (S)-1 differentially affects Kv7 (KCNQ) potassium channels. Neuropharmacology. 51(6):1068-77

Biervert C. Schroeder BC, Kubisch C, Berkovic SF, Propping P, Jentsch TJ, Steinlein OK (1998). A potassium channel mutation in neonatal human epilepsy. Science 279: 403-406

Bierbower SM, Watts LT, Shapiro MS (2011). M-type K+ channels: in vivo neuroprotective role during cerebrovascular stroke. 55th annual meeting of Biophysical society, Baltimore, March 5-9 .

Block F, Pergande G, Schwarz M (1997). Flupirtine reduces functional deficits and neuronal damage after global ischemia in rats. Brain Res. 754(1-2):279-84

Boscia F, Annunziato L, Taglialatela M (2006). Retigabine and flupirtine exert neuroprotective actions in organotypic hippocampal cultures. Neuropharmacology 51(2):283-94

Brenner R, Jegla TJ, Wickenden A, Liu Y, Aldrich RW (2000). Cloning and functional characterization of novel large conductance calcium-activated potassium channel beta subunits, hKCNMB3 and hKCNMB4. J Biol Chem. 275(9):6453-61

Brown DA, Adams PR (1980). Muscarinic suppression of a novel voltage-sensitive K+ current in a vertebrate neurone. Nature 283: 673-676.

Brown DA, Passmore GM (2009). Neural KCNQ (Kv7) channels. Br J Pharmacol. 156(8):1185-95

Castaldo P, del Giudice EM, Coppola G, Pascotto A, Annunziato L, Taglialatela M (2002). Benign familial neonatal convulsions caused by altered gating of KCNQ2/KCNQ3 potassium channels. J Neurosci. 22:RC199.

Catterall, W. A. (2010). Ion channel voltage sensors: structure, function, and pathophysiology. Neuron 67, 915–928.

Cha A, Bezanilla F (1997). Characterizing voltage-dependent conformational changes in the Shaker K+ channel with fluorescence. Neuron 19: 1127-1140.

Charlier C, Singh NA, Ryan SG, Lewis TB, Reus BE, Leach RJ, Leppert M (1998). A pore mutation in a novel KQT-like potassium channel gene in an idiopathic epilepsy family. Nat Genet. 18(1):53-5

Cooper EC1, Aldape KD, Abosch A, Barbaro NM, Berger MS, Peacock WS, Jan YN, Jan LY (2000). Colocalization and coassembly of two human brain M-type potassium channel subunits that are mutated in epilepsy. Proc Natl Acad Sci U S A. 97:4914-4919.

Cooper EC, Harrington E, Jan YN, Jan LY (2001). M Channel KCNQ2 subunits are localized to key sites for control of neuronal network oscillations and synchronization in mouse brain. J Neurosci. 21(24):9529-40

Costa C, Martella G, Picconi B, Prosperetti C, Pisani A, Di Filippo M, Pisani F, Bernardi G, Calabresi P. (2006). Multiple mechanisms underlying the neuroprotective effects of antiepileptic drugs against in vitro ischemia. Stroke. 37(5):1319-26

Colom LV, Diaz ME, Beers DR, Neely A, Xie WJ, Appel SH (1998). Role of potassium channels in amyloid-induced cell death. J Neurochem. 70(5):1925-34

Dalby-Brown W, Jessen C, Hougaard C, Jensen ML, Jacobsen TA, Nielsen KS, Erichsen HK, Grunnet M, Ahring PK, Christophersen P, Strøbæk D, Jørgensen S. Characterization of a novel high-potency positive modulator of K(v)7 channels (2013). Eur J Pharmacol. 709:52-63.

Dedek K, Kunath B, Kananura C, Reuner U, Jentsch TJ and Steinlein OK (2001). Myokymia and neonatal epilepsy caused by a mutation in the voltage sensor of the KCNQ2 K+ channel. Proc Natl Acad Sci 98: 12272-12277.

Devaux JJ, Kleopa KA, Cooper EC, Scherer SS. (2004). KCNQ2 is a nodal K+ channel. J Neurosci. 24(5):1236-44.

Delmas P, Brown DA (2005). Pathways modulating neural KCNQ/M (Kv7) potassium channels. Nat Rev Neurosci. 6(11):850-62.

Doyle KP, Simon RP, Stenzel-Poore MP (2008). Mechanisms of ischemic brain damage. Neuropharmacology 55:310–8.

Ekberg J, Schuetz F, Boase NA, Conroy SJ, Manning J, Kumar S, Poronnik P, Adams DJ. Regulation of the voltage-gated K channels KCNQ2/3 and KCNQ3/5 by ubiquitination. Novel role for Nedd4-2. J Biol Chem 282: 12135–12142, 2007.

Fanger CM, Ghanshani S, Logsdon NJ, Rauer H, Kalman K, Zhou J, Beckingham K, Chandy KG, Cahalan MD, Aiyar J (1999). Calmodulin mediates calcium-dependent activation of the intermediate conductance KCa channel, IKCa1. J Biol Chem 274: 5746– 5754.

Ficker E, Taglialatela M, Wible BA, Henley CM, Brown AM (1994). Spermine and spermidine as gating molecule for inward rectifier K+ channels. Science 266: 1068-1072.

Gamper N, Shapiro MS (2003) Calmodulin mediates Ca2+-dependent modulation of M-type K+ channels. J Gen Physiol. 122(1):17-31

Gamper N, Stockand JD, Shapiro MS (2003). Subunit-specific modulation of KCNQ potassium channels by Src tyrosine kinase J Neurosci. 1;23(1):84-95.

Gassen M, Pergande G, Youdim MB. Antioxidant properties of the triaminopyridine, flupirtine. Biochem Pharmacol. 1998;56(10):1323–1329.Geiger J, Weber YG, Landwehrmeyer B, Sommer C, Lerche H (2006). Immunohistochemical analysis of KCNQ3 potassium channels in mouse brain. Neurosci. Lett. 400, 101–104

Gruss M, Bushell TJ, Bright DP, Lieb WR, Mathie A, Franks NP (2004). Two-pore-domain K_ channels are a novel target for the anesthetic gases xenon, nitrous oxide, cyclopropane. Mol Pharmacol 65: 443–452.

Gunthorpe MJ, Large CH, Sankar R (2012). The mechanism of action of retigabine (ezogabine), a first-in-class K+ channel opener for the treatment of epilepsy. Epilepsia 53(3):412–424.

Gutman GA, Chandy KG, Grissmer S, Lazdunski M, McKinnon D, Pardo LA, Robertson GA, Rudy B, Sanguinetti MC, Stühmer W, Wang X (2005). International Union of Pharmacology. LIII. Nomenclature and molecular

relationships of voltage-gated potassium channels. Pharmacol Rev. 57(4):473-508

Haitin Y, Attali B (2008). The C-terminus of Kv7 channels: a multifunctional module.J Physiol. 586(7):1803-10.

Hansen HH, Ebbesen C, Mathiesen C, Weikop P, Rønn LC, Waroux O, Scuvée-Moreau J, Seutin V, Mikkelsen JD (2006). The KCNQ channel opener retigabine inhibits the activity of mesencephalic dopaminergic systems of the rat. J Pharmacol Exp Ther 318(3):1006-19.

Hedley PL, Jørgensen P, Schlamowitz S, Wangari R, Moolman-Smook J, Brink PA, Kanters JK, Corfield VA, Christiansen M (2009). The genetic basis of long QT and short QT syndromes: a mutation update. Hum Mutat. 30(11):1486-511

Heitzmann D, Warth R. (2008). Physiology and pathophysiology of potassium channels in gastrointestinal epithelia. Physiol Rev. 88(3):1119-82

Henshall DC, Simon RP. Epilepsy and apoptosis pathways (2005). J Cereb Blood Flow Metab.25(12):1557-72

Hermann R, et al. (2003) Effects of age and sex on the disposition of retigabine. Clin Pharmacol Ther 73(1):61–70.

Hernandez CC, Falkenburger B, Shapiro MS (2009). Affinity for phosphatidylinositol 4,5-bisphosphate determines muscarinic agonist sensitivity of Kv7 K channels. J Gen Physiol 134: 437–448

Hoshi N, Zhang JS, Omaki M, Takeuchi T, Yokoyama S, Wanaverbecq N, Langeberg LK, Yoneda Y, Scott JD, Brown DA, Higashida H (2003). AKAP150 signaling complex promotes suppression of the M-current by muscarinic agonists. Nat Neurosci. Jun;6(6):564-71.

Howard RJ, Clark KA, Holton JM, Minor DL Jr (2007). Structural insight into KCNQ (Kv7) channel assembly and channelopathy. Neuron.; 53(5):663-75.

Iannotti FA, Panza E, Barrese V, Viggiano D, Soldovieri MV, Taglialatela M (2010). Expression, localization, and pharmacological role of kv7 potassium channels in skeletal muscle proliferation, differentiation, and survival after myotoxic insults. J Pharmacol Exp Ther. 332(3):811-20

Isom LL, De Jongh KS and Catterall WA (1994). Auxiliary subunits of voltage-gated ion channels. Neuron 12: 1183-1194.

Jepps TA, Greenwood IA, Moffatt JD, Sanders KM, Ohya S (2009). Molecular and functional characterization of Kv7 K+ channel in murine gastrointestinal smooth muscles. Am J Physiol Gastrointest Liver Physiol. 297(1):G107-15

Jepps TA, Chadha PS, Davis AJ, Harhun MI, Cockerill GW, Olesen SP, Hansen RS, Greenwood IA (2011). Downregulation of Kv7.4 channel activity in primary and secondary hypertension. Circulation. 124:602-11

Jepps TA, Olesen SP, Greenwood IA (2013). One man's side effect is another man's therapeutic opportunity: targeting Kv7 channels in smooth muscle disorders. Br J Pharmacol. 168:19-27.

Jespersen T, Grunnet M, Olesen SP. The KCNQ1 potassium channel: from gene to physiological function. Physiology 20: 408–416, 2005.

Jia Q, Jia Z, Zhao Z, Liu B, Liang H & Zhang H (2007). Activation of epidermal growth factor receptor inhibits KCNQ2/3 current through two distinct pathways: membrane PtdIns(4,5)P2 hydrolysis and channel phosphorylation. J Neurosci. 27, 2503–2512.

Jiang, Y., Lee, A., Chen, J., Cadene, M., Chait, B. T., and MacKinnon, R. (2002a). Crystal structure and mechanism of a calcium-gated potassium channel. Nature 417, 515–522.

Jiang, Y., Lee, A., Chen, J., Cadene, M., Chait, B. T., and MacKinnon, R. (2002b). The open pore conformation of potassium channels. Nature 417, 523–526.

John CE and Jones SR. Fast Scan Cyclic Voltammetry of Dopamine and Serotonin in Mouse Brain Slices (2007). In: Michael AC, Borland LM, editors.

Electrochemical Methods for Neuroscience. Boca Raton (FL): CRC Press;. Chapter 4. Available from: http://www.ncbi.nlm.nih.gov/books/NBK2579/)

Kharkovets T, Dedek K, Maier H, Schweizer M, Khimich D, Nouvian R, Vardanyan V, Leuwer R, Moser T, Jentsch TJ (2006). Mice with altered KCNQ4 K+ channels implicate sensory outer hair cells in human progressive deafness.EMBO J. 25(3):642-52

Korsgaard MP, Hartz BP, Brown WD, Ahring PK, Strobaek D, Mirza NR (2005). Anxiolytic effects of maxipost (BMS-204352) and retigabine via activation of neuronal Kv7 channels. J. Pharmacol. Exp. Ther. 314, 282–292

Kubisch C, Schroeder BC, Friedrich T, Lütjohann B, El-Amraoui A, Marlin S, Petit C, Jentsch TJ. KCNQ4, a novel potassium channel expressed in sensory outer hair cells, is mutated in dominant deafness. Cell 96: 437–446, 1999.

Kupershmidt S, Snyders DJ, Raes A, Roden DM (1998). A K+ channel splice variant common in human heart lacks a C-terminal domain required for expression of rapidly activating delayed rectifier current. J Biol Chem. 16;273(42):27231-5.

Kuryshev YA, Gudz TI, Brown AM, Wible BA (2000). KChAP as a chaperone for specific K(+) channels. Am J. Physiol Cell Physiol.; 278(5):C931-41.

Lange W, Geissendörfer J, Schenzer A, et al (2009). Refinement of the binding site and mode of action of the anticonvulsant retigabine on KCNQ K+ channels. Mol Pharmacol. 75:272–280.

Leung YM. Voltage-gated K+ channel modulators as neuroprotective agents (2010). Life Sci. 86(21-22):775-80

Li M, Jan YN, Jan Li (1992). Specification of subunit assembly by the hydrophilic amino-terminal domanin of the Shaker potassium channel. Science 257: 1255-1230.

Li Y, Gamper N, Hilgemann DW, Shapiro MS (2005). Regulation of Kv7 (KCNQ) K channel open probability by phosphatidylinositol 4,5-bisphosphate. J Neurosci 25: 9825–9835.

Lieb K, Andrae J, Reisert I, Pilgrim C (1995). Neurotoxicity of dopamine and protective effects of the NMDA receptor antagonist AP-5 differ between male and female dopaminergic neurons. Exp Neurol. 134:222–9.

Long SB, Campbell EB and Mackinnon R (2005a) Crystal Structure of a Mammalian Voltage-Dependent Shaker Family K+ Channel. Science 309: 897-903.

Long SB, Campbell EB, MacKinnon R (2005b). Voltage Sensor of Kv1.2: Structural Basis of Electromechanical Coupling. Science 309: 903-908.

Ludwig J, Owen D, Pongs O (1997). Carboxy-terminal domain mediates assembly of the voltage-gated rat ether-a-go-go potassium channel. EMBO J 16: 6337-6345

Lundby A, Tseng GN, Schmitt N (2010). Structural basis for K(V)7.1-KCNE(x) interactions in the I(Ks) channel complex. Heart Rhythm 7: 708–713

MacKinnon R. (2004). Potassium channels and the atomic basis of selective ion conduction (Nobel Lecture). Angew Chem Int Ed Engl. 20;43(33):4265-77

Mannuzzu LM, Moronne MM, Isacoff EY (1996). Direct physical measure of conformational rearrangement underlying potassium channel gating. Science 271: 213-216.

Martire M, Castaldo P, D'Amico M, Preziosi P, Annunziato L, Taglialatela M (2004). M channels containing KCNQ2 subunits modulate norepinephrine, aspartate, and GABA release from hippocampal nerve terminals. J. Neurosci. 24, 592–597

Martire M, D'Amico M, Panza E, Miceli F, Viggiano D, Lavergata F, Iannotti FA, Barrese V, Preziosi P, Annunziato L, Taglialatela M (2007). Involvement of

KCNQ2 subunits in [3H]dopamine release triggered by depolarization and pre-synaptic muscarinic receptor activation from rat striatal synaptosomes. J Neurochem.102:179-193.

Matsuda H (1991). Magnesium gating of the inwardly rectifying K+ channel. Annu Rev Physiol 53: 289-298.

Miceli F, Soldovieri MV, Lugli L, Bellini G, Ambrosino P, Migliore M, del Giudice EM, Ferrari F, Pascotto A, Taglialatela M (2009).Neutralization of a unique, negatively-charged residue in the voltage sensor of K V 7.2 subunits in a sporadic case of benign familial neonatal seizures. Neurobiol Dis. 34:501-10

Miceli F, Soldovieri MV, Iannotti FA, Barrese V, Ambrosino P, Martire M, Cilio MR, Taglialatela M (2011). The Voltage-Sensing Domain of K(v)7.2 Channels as a Molecular Target for Epilepsy-Causing Mutations and Anticonvulsants. Front Pharmacol 1;2:2.

Nabbout R, Dulac O (2011) Epilepsy. Genetics of early-onset epilepsy with encephalopathy. Nat Rev Neurol 8(3):129–130.

Okada M, Zhu G, Hirose S, Ito KI, Murakami T, Wakui M, Kaneko S (2003). Age-dependent modulation of hippocampal excitability by KCNQ-channels. Epilepsy Res. 53(1-2):81-94.

Painter MJ, Sher MS, Stein AD, et al. Phenobarbital compared with phenytoin for the treatment of neonatal seizures. N Engl J Med. 1999;341(7):485–489.

Pan Z, Kao T, Horvath Z, Lemos J, Sul JY, Cranstoun SD, Bennett V, Scherer SS, Cooper EC (2006). A common ankyrin-G-based mechanism retains KCNQ and NaV channels at electrically active domains of the axon. J Neurosci. 8;26(10):2599-613.

Pannaccione A, Secondo A, Scorziello A, Calì G, Taglialatela M, Annunziato L. Nuclear factor-kappaB activation by reactive oxygen species mediates voltage-gated K+ current enhancement by neurotoxic beta-amyloid peptides

in nerve growth factor-differentiated PC-12 cells and hippocampal neurones (2005). J Neurochem. 94(3):572-86.

Pannaccione A, Boscia F, Scorziello A, Adornetto A, Castaldo P, Sirabella R, Taglialatela M, Di Renzo GF, Annunziato L. (2007). Up-regulation and increased activity of KV3.4 channels and their accessory subunit MinK-related peptide 2 induced by amyloid peptide are involved in apoptotic neuronal death. Mol Pharmacol. 72(3):665-73

Papazian DM, Schwarz TL, Tempel BL, Jan YN, Jan LY (1987). Cloning of genomic and complementary DNA from Shaker, a putative potassium channel gene from Drosophila. Science 237: 749-753

Papazian DM, Timpe LC, Jan YN, Jan LY (1991). Alteration of voltage-dependence of Shaker potassium channel by mutation in the S4 sequence. Nature 349: 305-310.

Passmore GM, Selyanko AA, Mistry M, Al-Qatari M, Marsh SJ, Matthews EA, Dickenson AH, Brown TA, Burbidge SA, Main M, Brown DA (2003). KCNQ/M currents in sensory neurons: significance for pain therapy. J Neurosci. 6;23(18):7227-36

Peretz A, Degani-Katzav N, Talmon M, Danieli E, Gopin A, Malka E, Nachman R, Raz A, Shabat D, Attali B (2007a). A tale of switched functions: from cyclooxygenase inhibition to M-channel modulation in new diphenylamine derivatives. PLoS One. 2(12):e1332.

Peretz A, Sheinin A, Yue C, Degani-Katzav N, Gibor G, Nachman R, Gopin A, Tam E, Shabat D, Yaari Y, Attali B. (2007b). Pre- and postsynaptic activation of M-channels by a novel opener dampens neuronal firing and transmitter release. J. Neurophysiol. 97, 283–295

Perozo E, Santacruz-Tolosa L. Stefani E, Bezanilla F, Papazian DM (1994). S4 mutations alter gating currents of Shaker K channels. Biophys J 66: 345-354.

Perozo E, Cortes DM, Cuello LG (1999). Structural Rearrangements Underlying K+-Channel Activation Gating. Science 285: 73-78.

Porter RJ, Nohria V, Rundfeldt C (2007). Retigabine. Neurotherapeutics. 4:149–154

Rasmussen HB, Frøkjaer-Jensen C, Jensen CS, Jensen HS, Jørgensen NK, Misonou H, Trimmer JS, Olesen SP, Schmitt N (2007). Requirement of subunit co-assembly and ankyrin-G for M-channel localization at the axon initial segment. J Cell Sci. 120:953-63.

Regev N, Degani-Katzav N, Korngreen A, Etzioni A, Siloni S, Alaimo A, Chikvashvili D, Villarroel A, Attali B, Lotan I (2009). Selective interaction of syntaxin 1A with KCNQ2: possible implications for specific modulation of presynaptic activity. PLoS One 4: e6586.

Roeloffs R, Wickenden AD, Crean C, et al. In vivo profile of ICA-27243 [N-(6-chloro-pyridin-3-yl)-3,4-difluoro-benzamide], a potent and selective KCNQ2/Q3 (Kv7.2/Kv7.3) activator in rodent anticonvulsant models (2000). J Pharmacol Exp Ther.326:818–828.

Rundfeldt C. The new anticonvulsant retigabine (D-23129) acts as an opener of K+ channels in neuronal cells (1997). Eur J Pharmacol.336:243–249.

Rundfeldt C. Characterization of the K+ channel opening effect of the anticonvulsant retigabine in PC12 cells (1999). Epilepsy Res. 35:99–107.

Sadewa AH, Sasongko TH; Gunadi, Lee MJ, Daikoku K, Yamamoto A, Yamasaki T, Tanaka S, Matsuo M, Nishio H (2008). Germ-line mutation of KCNQ2, p.R213W, in a Japanese family with benign familial neonatal convulsion. Pediatr Int. 50:167-71

Safiulina VF, Zacchi P, Taglialatela M, Yaari Y, Cherubini E (2008). Low expression of Kv7/M channels facilitates intrinsic and network bursting in the developing rat hippocampus. J Physiol. 586(22):5437-53

Saitsu H, Kato M, Koide A, Goto T, Fujita T, Nishiyama K, Tsurusaki Y, Doi H, Miyake N, Hayasaka K, Matsumoto N (2012). Whole exome sequencing identifies KCNQ2 mutations in Ohtahara syndrome. Ann Neurol. 72:298-300

Sanguinetti MC, Curran ME, Zou A, Shen J, Spector PS, Atkinson DL, Keating MT (1996). Coassembly of K(V)LQT1 and minK (IsK) proteins to form cardiac I(Ks) potassium channel. Nature. 384(6604):80-3

Sarna GS, Obrenovitch TP, Matsumoto T, Symon L, Curzon G (1990). Effect of transient cerebral ischaemia and cardiac arrest on brain extracellular dopamine and serotonin as determined by in vivo dialysis in the rat. J Neurochem. 55:937–40.

Schroeder bc, Kubisch C, Stein V and Jentsch TJ (1998) Moderate loss of function of cyclic-AMP-modulated KCNQ2/KCNQ3 K+ channels causes epilepsy. Nature. 396:687-690

Schroeder BC, Hechenberger M, Weinreich F, Kubisch C, Jentsch TJ (2000). KCNQ5, a novel potassium channel broadly expressed in brain, mediates M-type currents. J Biol Chem. 275(31):24089-95.

Schwake M, Pusch M, Kharkovets T, Jentsch TJ (2000). Surface expression and single channel properties of KCNQ2/KCNQ3, M-type K+ channels involved in epilepsy. J Biol Chem 275: 13343-13348

Schenzer A, Friedrich T, Pusch M, et al. Molecular determinants of KCNQ (Kv7) K+ channel sensitivity to the anticonvulsant retigabine (2005). J Neurosci.25:5051–5060.

Shao XM, Papazian DM (1993). S4 mutations alter the single-channel gating kinetics of Shaker K+ channels. Neuron. 11(2):343-52

Shieh CC, Coghlan M, Sullivan JP, Gopalakrishnan M (2000). Potassium channels: molecular defects, diseases, and therapeutic opportunities. Pharmacol Rev. 52:557-594

Simon DB, Karet FE, Rodriguez-Soriano J, Hamdan JH, DiPietro A, Trachtman H, Sanjad SA, Lifton RP (1996). Genetic heterogeneity of Bartter's syndrome revealed by mutations in the K_ channel, ROMK. Nature Genet 14: 152–156,

Singh NA, Charlier C, Stauffer D, DuPont BR, Leach RJ, Melis R, Ronen GM, Bjerre I, Quattlebaum T, Murphy JV, McHarg ML, Gagnon D, Rosales TO, Peiffer A, Anderson VE and Leppert M (1998). A novel potassium channel gene, KCNQ2, is mutated in an inherited epilepsy of newborns. Nat Genet 18: 25-29.

Singh NA, Otto JF, Dahle EJ, Pappas C, Leslie JD, Vilaythong A, Noebels JL, White HS, Wilcox KS, Leppert MF (2008). Mouse models of human KCNQ2 and KCNQ3 mutations for benign familial neonatal convulsions show seizures and neuronal plasticity without synaptic reorganization. J Physiol. 586(14):3405-23

Smith RJH, Hildebrand M. DFNA2 nonsyndromic hearing loss. In: GeneReviews, edited by Pagon RA, Bird TD, Dolan CR, Stephens K. Seattle, WA: University of Washington, Seattle, 2008.

Smith JS, Ianotti CA, Dargis P, Christian EP, Aiyar J (2001). Differential expression of KCNQ2 splice variants: implications to M-current function during neuronal development. J Neurosci 21: 1096–1103

Soldovieri MV, Miceli F, Taglialatela M. (2011) Driving with no brakes: molecular pathophysiology of Kv7 potassium channels. Physiology (Bethesda). 26:365-76.

Stamford JA (1990). Fast cyclic voltammetry: measuring transmitter release in 'real time'. J Neurosci Methods. 34:67–72.

Thomas P, Ye Y, Lightner E (1996). Mutation of the pancreatic islet inward rectifier Kir6.2 also leads to familial persistent hyperinsulinemic hypoglycemia of infancy. Hum Mol Genet 5: 1809–1812

Toner CC, Stamford JA (1996). 'Real time' measurement of dopamine release in an in vitro model of neostriatal ischaemia. J Neurosci Methods;67:133–40.

Toner CC, Connelly K, Whelpton R, Bains S, Michael-Titus AT, McLaughlin DP, Stamford JA (2001). Effects of sevoflurane on dopamine, glutamate and

aspartate release in an in vitro model of cerebral ischaemia. Br J Anaesth. 86:550-554.

Tzingounis AV, Heidenreich M, Kharkovets T, Spitzmaul G, Jensen HS, Nicoll RA, Jentsch TJ (2010). The KCNQ5 potassium channel mediates a component of the afterhyperpolarization current in mouse hippocampus. Proc Natl Acad Sci U S A. 107:10232-7

Wang Q, Curran ME, Splawski I, Burn TC, Millholland JM, VanRaay TJ, Shen J, Timothy KW, Vincent GM, de Jager T, Schwartz PJ, Toubin JA, Moss AJ, Atkinson DL, Landes GM, Connors TD, Keating MT (1996). Positional cloning of a novel potassium channel gene: KVLQT1 mutations cause cardiac arrhythmias Nat Genet. 12: 17–23

Wang HS, Pan S, Shi W, Brown BS, Wymore RS, Cohe IS, Dixon JE, McKinnon D (1998). KCNQ2 and KCNQ3 potassium channel subunits: Molecular correlates of the M-channel. Science. 282: 1890-1893

Weber YG, Geiger J, Kampchen K, Landwehrmeyer B, Sommer C, Lerche H (2006). Immunohistochemical analysis of KCNQ2 potassium channels in adult and developing mouse brain. Brain Res. 1077: 1–6.

Wen H, Levitan IB (2002). Calmodulin is an Auxiliary Subunit of KCNQ2/3 Potassium Channels. J Neurosci 18: 7991-8001.

Weckhuysen S, Mandelstam S, Suls A, Audenaert D, Deconinck T, Claes LR, Deprez L, Smets K, Hristova D, Yordanova I, Jordanova A, Ceulemans B, Jansen A, Hasaerts D, Roelens F, Lagae L, Yendle S, Stanley T, Heron SE, Mulley JC, Berkovic SF, Scheffer IE, de Jonghe P (2012). KCNQ2 encephalopathy: emerging phenotype of a neonatal epileptic encephalopathy. Ann Neurol. 71:15-25

Wickenden AD, Krajewski JL, London B, et al. N-(6-chloro-pyridin-3-yl)-3,4-difluoro-benzamide (ICA-27243): A novel, selective KCNQ2/Q3 potassium channel activator. Mol Pharmacol. 2008;73(3):977–986.

Wulff H, Castle NA, Pardo LA (2009). Voltage-gated potassium channels as therapeutic targets Nat Rev Drug Discov. 8(12):982-1001

Wuttke TV, Jurkat-Rott K, Paulus W, Garncarek M, Lehmann-Horn F, Lerche H (2007). Peripheral nerve hyperexcitability due to dominant-negative KCNQ2 mutations. Neurology. 69:2045–2053.

Xiong Q, Sun H, Li M (2007). Zinc pyrithione-mediated activation of voltagegated KCNQ potassium channels rescues epileptogenic mutants. Nat Chem Biol. 3:287–296.

Xiong Q, Sun H, Zhang Y, Nan F, Li M (2008). Combinatorial augmentation of voltage-gated KCNQ potassium channels by chemical openers. Proc Natl Acad Sci U S A.105:3128–3133.

Yu SP, Yeh CH, Sensi SL, Gwag BJ, Canzoniero LM, Farhangrazi ZS, Ying HS, Tian M, Dugan LL, Choi DW (1997). Mediation of neuronal apoptosis by enhancement of outward potassium current. Science. 278:114-117.

Yus-Najera E, Santana-Castro I, Villarroel A (2002). The identification and characterization of a noncontinuous calmodulin-binding site in noninactivating voltage-dependent KCNQ potassium channels. J Biol Chem. 277(32):28545-53

Zhou X, Wei J, Song M, Francis K, Yu SP. (2011). Novel role of KCNQ2/3 channels in regulating neuronal cell viability. Cell Death Differ. 18:493-505